NASA Contractor Report 3824

Color Measurement and Discrimination

Brian A. Wandell

COOPERATIVE AGREEMENT NCC2-44
FEBRUARY 1985

NASA

NASA Contractor Report 3824

Color Measurement and Discrimination

Brian A. Wandell
Stanford University
Stanford, California

Prepared for
Ames Research Center
under Cooperative Agreeement NCC2-44

National Aeronautics
and Space Administration

**Scientific and Technical
Information Branch**

1985

Abstract

Theories of color measurement attempt to provide a quantitative means for predicting whether two lights will be discriminable to an average observer. I consider color measurement theories of the following kind: Suppose the observer's state of adaptation is held fixed, and suppose lights a and b evoke responses from three color channels that we characterize as vectors, $v(a)$ and $v(b)$. The vector difference $v(a) - v(b)$ corresponds to a set of channel responses that would be generated by some real light, call it Δ. We expect a and b will be *discriminable* when Δ is *detectable.*

This paper reports a detailed development and test of the hypothesis that when the adapated state is held constant, the vector difference predicts the discriminability of pairs of lights. In the absence of a luminance component in the test stimuli, a and b, the theory holds well. In the presence of a luminance component, the theory is clearly false. When a luminance component is present discrimination judgments depend largely on whether the lights being discriminated fall in separate, *categorical* regions of color space.

Introduction

Color measurement

Quantitative measurement has progressed further in color vision than other disciplines within sensory psychology. For the simplest type of measurement, in which we attempt to decide whether two stimuli are visually *equivalent,* the science of color vision is a complete success. Just as methods within physics permit one to determine whether two objects -- however different in shape and material -- will be equivalent in weight, methods within color science permit one to determine whether two lights -- however different in their spectral energy distribution -- will be equivalent in appearance.

The notion of measurement includes more than the ability to identify equivalences among stimuli -- we must also be able to estimate the size of differences. In sensory psychology broadly, and color science specifically, the procedure for estimating color differences starts with the internal representation of the two stimuli that are to be discriminated. In the case of color, for example, we know that we can express each of the lights as a three-dimensional vector, say (a_1, a_2, a_3) and (b_1, b_2, b_3). If the observer's state of adaptation is held fixed, and the test lights a and b are weak and briefly presented so that the observer's state of adaptation is not disturbed, then it is generally assumed that the discriminability of a and b can be predicted from their vector

difference: (a_1 - b_1, a_2 - b_2, a_3 - b_3). The usual rule is to suppose that a and b will be *discriminable* if the light that would give rise to the vector difference a - b is *detectable.*

This theory of difference measurement assumes that non-linearities prior to the discrimination judgment are due to the observer's state of adaptation. Or put positively, the discrimination process is effectively linear when the state of adaptation held constant. A practical means of testing this hypothesis is to measure the discriminability of lights that are presented briefly and are but little different from the prevailing background illumination. These lights will not disturb the state of adaptation. Effectively, then, the observer judges differences among lights that are all within a small, local region of color space.

I call the hypothesis that discriminability can be estimated from knowing only the vector difference of the two lights the *vector difference hypothesis.* The vector difference hypothesis is a general measurement assumption, encompassing most types of measurement used in the physical sciences and most methods of measuring differences in sensory science. I have reviewed the hypothesis and the difficulties it has had in color vision measurement elsewhere (Wandell, 1982). The basic framework is being widely applied in other areas, such as in the discrimination of spatial patterns (Campbell and Robson, 1968; Sagi and Hochstein, 1984; Watson, 1984; Wilson and Gelb, 1984).

In this paper I report new results showing that under some adapting conditions,

and for test lights with slow temporal modulations, the vector difference hypothesis represents an adequate characterization of the data. For certain experimental conditions, then, *color measurement can be successfully extended to include a difference measure that predicts the discriminability of pairs of lights.*

There is a substantial failure of the theory when the temporal modulation of the test lights is increased to a range commensurate with the flicker introduced, say, by normal eye movements across borders and the test stimuli have a luminance component. In this case it is not possible to use the color discrimination experiment as a basis for color difference measurement. With flickering test stimuli containing a luminance component the visual system *abandons measurement in favor of stimulus categorization.*

The implication of this result extends beyond color measurement and includes sensory assessment of other stimulus attributes as well. Whenever a stimulus attribute must be estimated using an assumption about the image -- for example color estimates may be based upon the assumption of uniform illumination (Horn, 1974) -- the sensory system attempts to verify the assumption within the image. If the assumption is met, stimulus measurement may proceed. If the assumption fails, a more conservative, perhaps categorical, assessment is made of the stimulus.

Methods

General considerations. The most influential analysis of color discrimination is MacAdam's (1942, 1943) work in which the variability of color-match settings is used to estimate color-discriminability. This technique and subsequent analyses (Silberstein and MacAdam, 1945; Brown 1951, 1952) have been very valuable, but they suffer from important drawbacks as well. Most significantly the matching technique allows the subject to control the timecourse of the stimulus used in the discrimination judgment both by permitting the subject to freely adjust the intensity of the stimulus, and by permitting the the subject to freely view the bi-partite field. I have chosen instead to analyze color discrimination using a forced-choice paradigm with controlled stimulus timecourse. As we shall see, control of the timecourse is a crucial consideration.

Apparatus. The data were collected using a specially constructed Maxwellian view apparatus. The apparatus consists of three channels, differing only in the wavelength of the light they deliver to the observer. The apparatus is diagramed in figure 1.

Each channel has its own lamp (quartz-halogen type). The intensity of the lamp is controlled by a closed feedback circuit described below. The light from each bulb is first collimated, and then passed through an interference filter

(Baird-Atomic). The wavelengths of the filters used in all experiments reported here were 440nm, 540nm, and 650nm.

The narrow-band beam is split by a thin piece of glass, part of the beam falling directly on a photodiode (United Detector Technologies, pin-10), while the remainder continues to the observer. Before reaching the observer the beam passes through one of a set of a neutral density filters mounted on a wheel. The beam is then focussed on a pinhole, re-collimated, and joined together with the beams from the two other channels. The three beams are then passed through a field stop and the final Maxwellian lens.

The observer's position is held fixed at the focal point of the Maxwellian lens by means of a bite-bar attached to a vise whose position is adjustable in three-dimensions.

Feedback circuitry. The fraction of light diverted from the main beam gives rise to a current from the photodiode. The current is converted to a voltage signal by an amplifier attached directly to the photodiode. This voltage provides an estimate of the amount of (monochromatic) light in the beam. This voltage is compared with a voltage provided from a digital-to-analog signal controlled by a micro-processor. Based upon the difference between the desired signal level (from the micro-processor) and the actual signal (from the photodiode/amplifier) the control voltage to a voltage-programmable power supply (Hewlett Packard, model 6282A) governing the lamp intensity is

adjusted.

The intensity level of the bulbs were varied over time by varying the voltage from the microprocessor. The design is conceptually similar to the design described in Rosen et al. (1970). The non-linearities in the bulb, however, make this design useful only for moderate amplitude modulations (less than 20%) and for temporal frequencies below about 12 Hz. This is adequate for detection and discrimination experiments, but not as useful for studies requiring high levels of modulation for adaptation.

Stimuli. The stimuli in these experiments were all 1.85 deg spots presented upon a dark (zero) background.

Two different temporal waveforms were used for test stimuli. In one set of experiments the bulb intensities were modulated by a (roughly) Gaussian timecourse, with -5.0sd to + 5.0sd taken for one second. The luminance over time can be written as

$$L(t) = L_0 + C\exp - \left[\frac{t - .5}{.2}\right] \quad 0 < t < 1$$

where C is the contrast, and L_0 is the steady state luminance of the background field.

In a second set of experiments the bulb intensities were modulated by the product of this same Gaussian timecourse and a 6Hz sine-wave.

$$L(t) = L_0 + C\exp - \left[\frac{t - .5}{.2}\right]\sin(2\pi f 6t) \quad 0 < t < 1$$

This is commonly called a 6Hz Gabor function (Gabor, 1946). Figure 2 shows the intensity of the light at the observer's eye for each of these kinds of stimuli.

Calibration. The stimuli were calibrated before each experimental session. First, the electronic feedback circuit was calibrated so that the amount of light falling on the photodiode caused the amplifier to read 3.0 volts, chosen simply because it is a convenient voltage in the middle of the circuitry's operating range. In this way we assured ourselves that the circuitry would be operating in the same voltage range session to session. This voltage could be set to a precision of about 0.3 percent.

Second, the amount of light actually arriving the final Maxwellian image -- that is at the observer's cornea -- was measured by means of a separate photodiode/amplifier. This light level could be adjusted by means of a small neutral density wedge placed at the pin-hole indiciated in figure . Each channel was set to a repeatable voltage -- at the observer's eye -- measured to a

precision of about 1.0 percent.

The degree of modulation caused by a control signal was measured approximately every six weeks by displaying the signals measured at the feedback circuitry using an oscilloscope with storage capabilities (Tektronix 5111). These signals permitted us to assess the linearity of the system and the gain of the apparatus. The calibration data were kept in a computer file and the latest calibration values were (automatically) used by the programs that estimated thresholds.

Error analysis. The response of the system is subject to two kinds of errors. The first types of errors are the non-linearities in the circuit, the principal difficulty arising from the bulb. Measurements were restricted to amplitudes and frequencies at which non-linearities could not be detected with the calibration equipment. The second types of errors are sampling errors introduced by the temporal sampling of the signal, and the discretization of the control signal amplitude within the range of 256 available levels.

The temporal sampling rate was kept constant at 10 ms (100 Hz). At this sampling rate temporal aliasing below 50Hz will not occur. (That is, the Nyquist limit for sampling at 100Hz is 50Hz). Since the bulb had no measurable response to signals beyond about 30Hz, the temporal sampling did not introduce significant distortions.

Over the varying experimental conditions it is not possible to use the full range of 256 sampling levels for every stimulus. Under some conditions threshold level signals may be represented by as few as 5 intensity levels. Of particular interest here is the degree of distortion introduced in the frequency domain at this level if intensity sampling. The relative energy spectrum of a signal with 256 levels differs by less than 1% from a signal sampled at 10 contrast levels. The contrast sampling does not introduce a significant stimulus artifact.

Detection threshold estimation procedure. Thresholds were measured using a two-alternative, forced-choice, multiple-staircase design. The initial stimulus level was set by hand to a contrast level at which the stimuli were judged barely, but regularly, detectable. Starting near this level four independent staircases were run in each block, each staircase continuing for 25 trials. The staircase rule was as follows: after each incorrect response increase the contrast of the signal by 2db, after two correct responses decrease the contrast of the signal by 2db.

Threshold estimates are generally based upon two or three sessions, for a total of 200-300 observations per data point. A single psychometric function was fit to the data pooled across sessions. The Weibull (see Quick, 1974) was used for its convenience and theoretical significance (Maloney and Wandell, 1983a)

$$P(cor) = \frac{1}{2} + \frac{1}{2} \exp - [\frac{C}{\alpha}]^{\beta}$$

where C is the stimulus contrast. At the contrast level α the observer is correct on 81 percent of the trials, and this value is plotting as threshold.

The data were fit to the Weibull using a maximum likelihood procedure described by Watson (1979). The fitting procedure has been analyzed by Maloney and Wandell (1983b) using a bootstrap simulation method. Maloney and I found that estimates of the intensity level at which 81% probability correct is obtained are stable (plus or minus one standard error) to within about 5 percent (linear intensity) using the fitting procedure based on 200 forced-choice observations. Further, for the stimuli used in this study, the value of the parameter β is always very near two.

Discrimination threshold estimation procedures. In the discrimination measurements the observer is presented with a weak pedestal light, Π , and a pedestal light plus an increment, $\Pi + \Delta$. The observer must identify which of the intervals contained the pedestal plus increment.

In these experiments only the contrast of the increment Δ is varied. The same staircase rule is followed as in the detection procedure. Two correct discriminations leads to a reduction in the contrast of the increment, any error

leads to an increase in the increment. The detection threshold experiment may be viewed as the special case of the discrimination experiment in which the pedestal light, Π , is zero.

The representation.

Results are plotted using a linear co-ordinate system. Each axis represents the linear intensity of a primary light. The data in figure 3 plots the intensity of the 650 nm channel on the horizontal axis and the intensity of the 540 nm channel on the vertical axis. The origin of the graph is at the *steady* level. The steady level establishes the state of adaptation. The absolute quantal levels of the adapting lights are indicated in the figure captions.

The modulations of the test lights at threshold are plotted on the graph at the *maximal contrast* of the stimulus during its presentation. The maximal contrast of the stimulus is computed as follows. Let the value of the intensity at its largest deviation from steady be I_p, and let the steady state intensity be I_0. Then the maximal stimulus contrast is

$$\frac{I_p - I_0}{I_0}$$

Symmetry of Gabor functions. When using the 6Hz Gabor function a shift from positive to negative contrast is equivalent to a shift of 180 degrees in the sinusoidal term. Such a shift is of no visual significance, so that the detectability of a 6Hz Gabor function plotted in the upper right quadrant, with

both contrast terms positive, will always be the same as the detectability of a 6Hz Gabor function in the lower left hand quadrant, where both contrasts are negative. This forces a symmetry on the 6Hz Gabor data that is not present in the Gaussian data. I took advantage of this symmetry and made measurements only between 0 and 180 degrees (measuring counter-clockwise from the x-axis) for 6Hz Gabor stimuli. The detection data points are plotted twice, however, for easier comparison with the Gaussian threshold measurements.

Gaussian perturbations.

Using these conventions, figure 3 represents the *detection contour* of a Gaussian perturbation of the adapting field. The adapting field in this condition was metameric to a 630 nm light.

Test inhibition. Two properties of the detection contour are striking. First, consider the upper right hand quadrant. In this quadrant the experiment consists of measurement of test additivity between two positive Gaussians (luminance increment). There is a clear inhibition between 540nm and 650nm modulations: Admixing 650nm test light to 540nm test light makes the 650nm test light less visible.

In the lower left hand quadrant we measure mixtures of pairs of decrements (luminance decrement). Again the data show that over a significant range there is a strong inhibition between the 650nm and 540nm decrements.

This inhibition is among the strongest reported in the literature (cf. Thornton and Pugh, 1983).

Mechanism linearity. A second significant property is that using the Gaussian timecourse, the detection contour is quite elongated. The data may be viewed as either falling along a very eccentric ellipse, or as having two sides that are roughly linear. The approximate linearity of the sides is expected on the assumption that the underlying mechanisms are linear near threshold. The linearity will only be revealed, however, when one of the mechanisms has generally much greater sensitivity.

If the underlying detection mechanisms are linear, we also expect that the data will fall symmetrically about the origin, as they do. The linearity of the sides and the symmetry about the origina is replicated in the detection contours of all of the observers we have tested. Data from several observers is shown in figure 4. The detection contours of the various observers measured in this experiment are in quite close quantitative agreement.

6Hz Gabor perturbations.

In figure 5 I have plotted the detection contour of the 6Hz Gabor timecourse and the detection contour of the Gaussian timecourse on a common axis.

Test additivity. Unlike the Gaussian data, the mixture of a 6Hz 540nm and 650nm lights do not inhibit. The 6Hz Gabor detection contour is considerably less elliptical, having none of the extended contours as in the Gaussian data. The increased circularity is replicated in all of the observers in figure 6

A common working hypothesis (Kelly and Van Norren, 1977; Guth et al., 1969, Ingling, 1981; Wandell and Pugh, 1980) is that the absence of test inhibition and change in sensitivity in the 45 degree direction occurs because of a luminance channel sensitive to flicker in the 45-225 degree directions, but insensitive to the Gaussian perturbation. The 6Hz Gabor data reveal the luminance mechanism and conceal the linear threshold contour of the opponent mechanism. [1]

Estimated spectral sensitivities

In the appendix (part a) I describe a theory of visual detection for the data presented in the previous section. The theory assumes that within the two-dimensional stimulus space used here threshold is mediated by probability summation among two independent, linear, visual channels. Appendix (part b) describes how the maximum likelihood detection contours -- plotted with the data points in the previous figures -- are computed. Appendix (part c) describes how the fitting of the detection contours provides a means of estimating the spectral sensitivity of each channel for wavelengths between 540nm and 650 nm.

The calculations and theory are presented on the assumption that there are but two mechanisms mediating threshold under these conditions. The present results do not permit us to decide on the number of mechanisms involved: other methods, such as detection/discrimination (Kirk, 1982; Wandell, Sanchez and Quinn, 1982) are required to address this issue. My purpose in providing the Appendix is to make available a method that is useful in relating the detection contours measured using test mixture experiments and the classic spectral sensitivity curves. As will be clear from an inspection of the procedure, it can be easily generalized to higher dimensions. The quantitative procedure is given in detail in the Appendix, and I describe the results based on the assumption of but two mechanisms in the following section. The analysis was performed on the assumption that two mechanisms mediate threshold because virtually no improvement in the fit is obtained by assuming a third mechanism contributes to sensitivity under the measurement conditions used here.

Gaussian test spectral sensitivities. The Gaussian test stimulus yields detection contours that are long in one direction and short in the other. The long side permits a good estimate of the slope of one detection channel, and thus its spectral sensitivity. The spectral sensitivity estimated from the short side is somewhat less reliable.

The long direction is oriented towards 45 degrees and thus will have an

opponent sensitivity (see appendix c). The short direction is oriented in roughly the 135 degree direction and will have a non-opponent sensitivity. The estimated spectral sensitivities of the two channels, averaged across all observers are plotted in figure 7. The data from each observer, separately, follow the same pattern.

The spectral sensitivity of the opponent-channel plausibly corresponds to the spectral sensitivity of the red-green opponent channel defined by the color cancellation experiment, a method based upon perceptual hue judgments. Under neutral adaptation conditions estimates from the color cancellation experiment (Hurvich and Jameson, 1955; Larimer, et al., 1974) place the equilibrium point of the red-green opponent channel near 570 nm. Under strong, long-wavelength chromatic adaptation the equilibrium point shifts to higher wavelengths (Larimer, 1981). The spectral sensitivity estimates here are consistent with these reports as the adapting field in these experiments is visually equivalent to a 630nm light, and the estimated equilibrium point is shifted to approximately 605nm for all observers.

The non-opponent spectral sensitivity peaks at too high a wavelength to plausibly describe the luminance channel. If it corresponds to a channel defined by perceptual judgments, it is likely to correspond to the yellow side of the blue-yellow opponent channel.

Gabor test spectral sensitivities. With the exception of a single spectral sensitivity curve, described later, the spectral sensitivities using the 6Hz Gabor are similar across observers. The averaged results are plotted in figure 8. The most sensitive wavelength for both of the channels estimated using the 6Hz Gabor function are at a wavelength slightly longer than the peak of the CIE luminosity function, though the secondary channel (filled symbols) cannot be estimated reliably because it does not dominate the detection in any part of the spectrum. It is possible that this channel -- were it revealed more completely -- would have the spectrum of the luminosity function. It is also possible that this channel is not unitary, but can be further decomposed. The problem of testing the unitary nature of these channels cannot be fully addressed here.

The data from the secondary channel of observer bw differ from the data from the other three observers. These results are plotted in figure 9. This observer's secondary channel is qualitatively different from the other observers, and thus was not included in the average. The opponency of this channel is identical to the opponency estimated for all observers using the Gaussian test spot. For this observer the only difference between the channels estimated using the Gaussian and Gabor functions is the relative sensitivity: using the Gabor function the sensitivity of the non-opponent channel is increased compared to the opponent channel.

Intermediate Discussion

Color difference measurement. With the fundamental structure established, I now turn to the problem of color measurement and color discrimination. The question I pose is to what extent can we predict the discriminability of pairs of lights not too different in intensity from the adapting field. The question is posed graphically in figure 10.

The simplest answer to this question, offered by the vector difference hypothesis, is that a will be *discriminable* from b when the differential responses they cause in the visual mechanisms is *detectable.* This prediction may be put concretely in terms of the visual mechanisms as follows.

Suppose that the response to light a is mediated principally by two channels, and we represent this response as $[C_1(a), C_2(a)]$. The response to light b will then be $[C_1(b), C_2(b)]$. The differential response to the two lights is given as the vector difference, $[C_1(a) - C_1(b), C_2(a) - C_2(b)]$. There is a real light, call it Δ, that would have given rise to this differential response (represented in figure 10 as the dashed vector). If the light Δ is detectable, then according to classic color measurement theory the lights a and b will be discriminable.

Since the detection contour defines the contrast of the physical stimulus required for a just detectable perturbation of the visual mechanisms, according to theory we should be able to predict the discriminability of lights by determining whether the difference vector Δ falls inside or outside this contour.

The vector difference hypothesis is independent (up to an arbitrary, invertible, linear transformation) of the co-ordinate system in which the stimuli are represented. To see this, suppose that Δ represents a detectable light in one co-ordinate system, so that in this co-ordinate frame two lights with a vector difference $a - b = \Delta$ will be discriminable. If we represent the lights in a new co-ordinate system, differing by a linear transformation T, then $T\Delta$ is the same light, so it is detectable. The new representations for a and b are Ta and Tb, and their vector difference is $Ta - Tb = T(a - b) = T\Delta$, so they again will be predicted to be discriminable.

II. Discrimination

Representation

The discrimination thresholds are plotted as pairs of points following the same conventions and using the same axes as the detection thresholds. One of the points (plotted as an open symbol) represents the pedestal ,Π , and the second point (plotted as a filled symbol) represents the pedestal plus increment, $\Pi + \Delta$, at which discrimination occurs at the .81 probability correct level. The vector difference between the two lights represents the increment alone, Δ. By the vector difference hypothesis the length of the difference vector must be constant independent of the pedestal (when the pedestal is a weak perturbation of the adapting field), and equal to the length of the vector at detection threshold.

Gaussian perturbations

One set of discrimination thresholds is plotted in figure 11. The pedestal points (open symbols) fall along a straight line at 22.5 degrees angle to the x-axis. These points fall on a perfectly straight line because they are chosen by the experimenter. With each pedestal point there is an associated pedestal plus increment (filled symbols), separated from the pedestal by a difference vector oriented 135 degrees (counter-clockwise) relative to the x-axis. The points

defining the pedestal plus difference fall closely parallel to the line of points defining the pedestal, indicating that the size of the difference vector is approximately constant, and independent of the pedestal. Under these stimulus conditions the vector difference hypothesis is satisfied.

Figure 12 plots further tests of the vector difference hypothesis using the Gaussian perturbations of the field. The pedestals fall along straight lines on the x-axis, and 45 degrees below x-axis. In all measurements the test vector is oriented at 135 degrees to the x-axis. The pedestal lines and the associated pedestal plus increment lines are approximately parallel as required by the vector difference hypothesis.

For the 13 discrimination measurements in figures 11 and 12, the mean value of the difference vector is a contrast of 2.54 percent with a standard deviation of .3 percent (standard error of the mean = .09 percent). Of the thirteen measurements only one point lies more than two standard deviations from the mean (-2.17 sd). These measurements do not permit us to reject the hypothesis.

A further test. In figure 13 I plot a further test of the hypothesis. In the previous test the pedestal was varied for each discrimination threshold and the increment was constant. In this test the pedestal is constant and the direction of the increment is varied. By sweeping out the discrimination thresholds for different directions of the increment we create *discrimination contours* in analogy

to the detection contour (the special case in which the pedestal light is zero). We expect, on the vector difference hypothesis, that the discrimination contours will have the same geometric shape as the detection contours.

In panel a of the figure I plot the detection contour along with the discrimination contours represented around their respective pedestal lights. Panel b of the figure represents the same data, but with the discrimination contours slid so that the pedestal lights are at the origin. This is done to facilitate comparison of the different shapes. Figure 14 displays a replication of these data on a second observer.

Under these conditions the data are generally consistent with the vector difference hypothesis. Although there may be some small, measurable differences, (particularly in for test lights in the 45 degree direction) the hypothesis serves as an excellent first order approximation to the large potential set of discrimination judgments.

I have already shown, however, (Wandell, 1982) that the vector difference hypothesis does not hold under all measurement conditions. In the next section I show that the timecourse of the lights is crucial in determining whether the hypothesis can succesfully describe the data

Discriminations with a 6Hz Gabor function

In figure 15 I plot discrimination thresholds using the 6Hz Gabor functions. As in the Gaussian data, pedestal positions fall along straight lines: in panel (a) the angle is 22.5 degrees, panel (b) 45 degrees and panel (c) 67.5 degrees. In all three panels the increment was in the 135 degree direction.

Categorization of stimulus regions. Figure 15 demonstrates a clear failure of the vector difference hypothesis. In panel a the length of the difference vector separating the pedestal and pedestal plus increment increases with the contrast of the pedestal. This trend is slightly evident in panel b and not evident in panel c. The failure is quite regular and predictable.

In figure 16 I have plotted all of the pedestal plus increments data points from figure 15 . These points fall approximately along a common line in stimulus co-ordinate space, despite the fact that the pedestals they are being discriminated from fall across a fairly wide range of stimulus space. This plot reveals that the *contrast of the incremental term is not critical* when predicting whether two lights will be discriminable. For example, discrimination thresholds measured from the 22.5 degree line can be as much as 2.5 times greater than the discriminations made along the same line, but measured starting from the 67.5 degree direction. The key factor in determining discriminability appears to be whether the two lights fall in a common or separate region of color space. It is the *visual system that defines where this*

border falls.

The same type of deviation can be seen for a second observer, using a 6Hz Gabor function, but a different adapting point, pedestal, and test directions. These are plotted in figure 17. The common border is illustrated in figure 18. I have replicated this pattern of discrimination results under various adapting conditions with various combinations of pedestal and increment.

The failure of the vector difference hypothesis occurs for lights that are at detection threshold. It is unlikely that the failure of the vector difference hypothesis is simply due to a loss of sensitivity caused by the pedestal. For measurements in some pedestal directions there is no loss of sensitivity with pedestal contrast. This is illustrated in figure 19 which is a set of discrimination thresholds in various directions around a pedestal in the 22.5 degree direction.

Figure 19 plots a detection contour and a discriminations around a pedestal position at 22.5 degrees. The patterns of discriminations are quite different from the pattern of detections, again indicating a failure of the vector difference hypothesis. The failure is such that test sensitivity in the 135 degree direction is decreased, while sensitivity in the 315 degree direction is essentially unchanged. The pattern of results is consistent with the idea that discrimination of increments *away from the principle direction of the pedestal* show categorical performance limits.

Nature of the visual mechanisms

There can be no doubt that there is a dramatic shift in discrimination behavior as the timecourse of the stimulus is varied. In analyzing the detection data I argued that differences in the properties of the detection contour occur because detection is mediated by different visual mechanisms when using the Gaussian versus 6Hz Gabor timecourses. This may also be the reason for the shift in discrimination performance. In particular, if the 6Hz Gabor function is a potent stimulus for a luminance mechanism, the shift in discrimination behavior may be due to a role played by the luminance channel.

To test this hypothesis I have measured the discriminability of 6Hz Gabor functions modulated entirely within the iso-luminance plane. In this way discrimination behavior among 6Hz Gabor functions cannot depend upon the response of the luminance mechanism. The detection and discrimination contours for such iso-luminance data are plotted in figure 20 The co-ordinate system used in this plot is also a stimulus based co-ordinate system, as in the previous plots. The degree of contrast modulation for two of the test stimulus channels are plotted explicitly as the horizontal and vertical axes. The contrast of the third test channel may be inferred from the contrast of the other two, as this contrast is determined by the fact that the total stimulus must be kept in the iso-luminance plane.

In figure 21 I plot the detection and discrimination contours slid so that the pedestals fall on the origin. The agreement in shape here is about as good as the agreement found using the Gaussian stimulus, and far better than the agreement found using the 6Hz Gabor unconstrained to fall in the iso-luminance plane. The 6Hz Gabor data measured with no luminance component are consistent with the vector difference hypothesis. These data support the view that categorization of discrimination responses occurs because of a role played by a luminance mechanism.

Conclusions

When discrimination depends principally upon opponent channels responses, discrimination thresholds can be predicted from the detection contour alone. This observation is consistent with a classic view of color measurement of small color differences that is described in the vector difference hypothesis.

Under conditions in which the luminance mechanism is significantly excited we find that discrimination judgments have a categorical quality. In this case it is not simply the size of the differential response among visual mechanisms that determines if two lights will be discriminable, but rather whether the differential responses fall on different sides of a boundary set by the visual system in color space.

The vector difference hypothesis asserts that there is a smallest *detectable perturbation* and that all detection and discrimination judgments work at this

resolution limit. Categorical responses, however, represent a different type of limit on discriminability. Differences that exceed this resolution limit are ignored if they do not cross a boundary imposed by visual processing. Two reasons for adopting this processing method are the following.

First, categorical limits may provide a means of focusing visual processing on those channels where dynamic stimulus events are clearly signaled. If estimating the perturbation of a channel containing a clear signal may take precedence over monitoring weaker perturbations in a second channel, then using a categorical limit reduces processing of the secondary channel since no variations in the secondary channel will be attended to until the response exceeds cross some fixed value. If this hypothesis is true, the results here suggest that automatic allocation of attention may occur between luminance and chromatic channels, but not between chromatic channels.

Second, the estimation of spectral properties of surfaces must depend upon some assumptions concerning the distribution of surface boundaries and ambient lighting conditions. Comparison of colors against different backgrounds or under spatially and temporally varying lighting conditions cannot proceed with the same fine grained level of measurement as under conditions in which the background surface and lighting conditions are constant. If luminance signals are used to indicate whether or not the physical environment meets the assumptions required for accurate visual estimation of spectral information, then the method of assessing color differences will shift

when luminance components are introduced into the test stimuli.

Appendix

A: Theory of channel detection mechanisms

Many empirical and theoretical methods have been described for extracting color channel sensitivity from test sensitivity data. There is something of a consensus among recent theoretical papers (see e.g. Boynton et al., 1964; Kranda and King-Smith, 1979; Maloney and Wandell, 1983a; Stiles, 1967) as to the elements of a theory of test sensitivity. First, the basic channels are described as responding linearly to small perturbations of the adapting field. Second, the channel output is assumed to have added noise. Third, the channel responses are combined by a probability summation rule based on a high-threshold assumption.

The analysis I report here is based upon this set of ideas. The analysis extends previous work in two ways. On the empirical side, since the data reported here include negative as well as positive Gaussians, the visual channel sensitivities are revealed over a wider range. On the theoretical side, I will provide a geometric interpretation of the results that unifies the detection contour measurements in the previous section with the spectral sensitivity of the underlying channels. [2]

Channel responses. The probability of a single channel signaling the presence of a stimulus depends on stimulus contrast as the Weibull psychometric function:

$$P(\textit{detect}) = 1 - \exp - [\frac{C}{\alpha_i}]^{\beta}$$

where C is the contrast of the test, and α_i is the i^{th} channel's sensitivity to the test. I adopt the high-threshold assumption that the chance of a channel signaling a stimulus is zero when no stimulus is present.

The chance of a correct detection response in a two-interval forced-choice design based upon a single-channel is

$$P(\textit{cor}) = \frac{1}{2} + \frac{1}{2}\exp - [\frac{C}{\alpha_i}]^{\beta}$$

A theoretical analysis of this psychometric function is provided in several places (Quick, 1974; Green and Luce, 1975; Wandell and Luce, 1978; Maloney and Wandell, 1983a).

Probability summation. When two channels contribute to the visibility of a test light, I assume that the observer responds correctly if at least one of the

channels indicates the presence of a signal. Using this probability summation rule the chance of a correct response is

$$P(cor) = \frac{1}{2} + \frac{1}{2}\exp - [\frac{C}{\alpha}]^{\beta}$$

where

$$\alpha = [(\alpha_1)^{\beta} + (\alpha_2)^{\beta}]^{\frac{1}{\beta}}$$

Co-ordinate systems. Consider the special co-ordinate system plotted in figure 22. In this plot the axes represent the theoretical channel responses. Sets of iso-sensitivity lines for each channel alone are the light, dashed lines parallel to the axes. The iso-sensitivity contour for detection using a probability summation between the two channels (with β two) is the heavy, dashed circle. I refer to this co-ordinate system as the *channel co-ordinate* system to distinguish it from the *stimulus co-ordinate system* used to represent the data. The two co-ordinate systems are related by a linear transformation, so that the circular iso-detection curves in the channel co-ordinate system plots as an ellipse in stimulus co-ordinates.

B: Maximum likelihood estimation of fitting detection contours

The purpose of this section of the appendix is to describe the computation of the maximum likelihood fit of the model to the observed results. The observations are collected in stimulus co-ordinates, where a stimulus is represented by its contrast on the 650nm and 540nm channels. Using vector notation we write $C = [C_{650}, C_{540}]$. For each pair of stimuli contrasts the data consist of a number of correct n_c and incorrect n_e forced-choice responses.

The theoretical problem is to discover the linear transformation from the stimulus co-ordinate system into the channel co-ordinate system that maximizes the likelihood of observing the data. We may represent the linear transformation as a 2x2 matrix that maps the vector C into a new vector, M, in channel co-ordinates.

$$\begin{bmatrix} X_{11} & X_{21} \\ X_{12} & X_{22} \end{bmatrix} \begin{bmatrix} C_{650} \\ C_{540} \end{bmatrix} = \begin{bmatrix} M_1 \\ M_2 \end{bmatrix}$$

The sensitivity of each channel is unity in the new co-ordinate frame. The predicted probability correct, given two channel responses $[M_1(a), M_2(a)]$ is given by the probability summation formula ($\beta = 2$) as

$$P(cor) = 1. - \exp\text{-}[M_1(a)^2 + M_2(a)^2]^{\frac{1}{2}}$$

Following the logic described in Watson (1979), we assume a binomial error distribution for the two-alternative forced-choice experiment. We compute the likelihood of observing n_c correct and n_e incorrect responses when the expected probability correct is p as

$$\begin{bmatrix} n_c + n_e \\ n_c \end{bmatrix} p^{n_c} (1 - p)^{n_e}$$

For computational precision it is best to maximize the log likelihood. Therefore we form the sum of the logarithms of the likelihood values across all stimuli, to obtain the log likelihood of the complete data set assuming the linear transformation parameters, X_{ij}. The maximum likelihood is found by an iterative search procedure (Chandler, 1965) over these parameters.

C: Determining channel spectral sensitivity

Axis orientation in stimulus co-ordinates. The maximum likelihood fit of an ellipse to the data in stimulus co-ordinates defines a linear transformation from

channel co-ordinates into stimulus co-ordinates. From this linear transformation we may determine the orientation of the channel axes plotted in stimulus co-ordinates. (These will not, in general, be the major and minor axes of the ellipse which are constrained to be orthogonal.) In stimulus co-ordinates the iso-sensitivity lines of each channel may be plotted along lines of the form

$$C_{540} = \tan(\theta_x) C_{650} + \textit{constant}$$

$$C_{540} = -\tan(\theta_y) C_{650} + \textit{constant}$$

where θ_x is the angle of rotation for the x - *axis* defining channel 1 in channel co-ordinates to stimulus co-ordinates, and θ_y is the angle of rotation for the y - *axis*, defining channel 2 from channel co-ordinates to stimulus co-ordinates. The C_i terms are the stimulus co-ordinates defining the amount of contrast in each primary light. For the data shown in figure 22 one channel's is oriented at 46 degrees (counter-clockwise) and the second channel has iso-sensitivity lines falling at 162 degrees (counter-clockwise).

Channel spectral sensitivity. The slope of the channel axes in stimulus co-ordinates permit us to determine the *spectral sensitivity* of each channel for lights with wavelength between the stimulus primaries of 650 nm and 540 nm. The

lines describe a spectral sensitivity function because each mixture of these particular primaries is metameric to a monochromatic light; that is, in this region the spectrum falls along a straight line in CIE co-ordinates. If the intensities of the primaries required for a metameric match to a light λ are $R_{540}(\lambda)$ and $R_{650}(\lambda)$, then the estimated relative spectral sensitivity of λ is

$$S_1(\lambda) = \frac{1}{R_{540}(\lambda) - \tan(\theta_x)R_{650}(\lambda)}$$

$$S_2(\lambda) = \frac{1}{R_{540}(\lambda) + \tan(\theta_y)R_{650}(\lambda)}$$

The computation may be performed in the following steps. First, for each ray oriented between 0 and 90 degrees from the origin, determine the point of intersection with one of the channel's unit iso-sensitivity line (i.e. the intercept equals 1 or -1). Second, for each such point, compute the effective wavelength by comparing its chromaticity co-ordinate (the normalized color-matching co-ordinate) with the chromaticity co-ordinates of spectral lights (see Wyszecki and Stiles, 1967, p. 240). Third, compute the effective contrast by taking the ratio of the length of the color matching function co-ordinates of the point and the length of the color-matching co-ordinates for the standard CIE color match to an equivalent monochromatic light of (unit) radiance. Finally, the spectral

sensitivity curve is simply the inverse contrast as a function of wavelength, with the caveat that when the ray intersects the iso-sensitivity line with positive unit sensitivity the contrast is plotted positively, and otherwise negatively.

Properties of the fit. The spectral sensitivity curves estimated in this way will have the following properties. First, all are linear transformations of the pigment sensitivities since they are based upon linear transformations of the color matching functions. Second, when channel axes fall at an angle of between 90 and 180 degrees (measured counter-clockwise from the x-axis) in stimulus co-ordinates, detection of all combinations of increments will be mediated by an iso-detection line with positive y-intercept. The spectral sensitivity estimate of the channel will, therefore, be positive. If the iso-sensitivity lines fall at an angle of between 0 and 90, then for some test directions threshold will be mediated by a line with positive y-intercept and for other directions by a line with negative y-intercept. We denote this difference by plotting the spectral sensitivity as positive or negative depending on the sign of the y-intercept of the iso-detection contour mediating detection. For orientations between 0 and 90 degrees, therefore, the channel will have an opponent sensitivity.

Footnotes

This work was supported by grant no. 2 RO1 EY03164 from the National Eye Institute, contract F33615-82-K-5108 from the Air Force, and grant no. NASA - NCC-2-44 from the National Aeronautics and Space Administration. I thank J. Farrell, G. Loftus, L. Maloney and E. Markman for their comments on the manuscript.

1. A clear example expressing the view that flickering lights cause a luminance response may be found in Guth et al. (1969).

> We have long theorized that judgments made in a flicker photometric situation are mediated by the non-opponent system. This is almost self-evident, since flicker photometry demands that judgments of minimum flicker be made after chromatic fusion has occurred. That is, the procedure is presumably dependent upon the fact that the non-opponent system is temporally more sensitive than the chromatic system (p. 568).

2. The theoretical development presented here is based on a theory of the behavior of individual channels described by Maloney and Wandell (1983a). Justifications for the assumptions are provided in that work.

Figure Captions

Figure 1. Schematic diagram of one of three channels of the experimental apparatus. See text for explanation.

Figure 2. Temporal waveforms of Gaussian (top) and 6Hz Gabor function (bottom). The horizontal axis is time (secs) and vertical axis is linear intensity.

Figure 3. Gaussian detection contour for observer bw. The mean adapting level (origin of the graph) is a mixture of 650 nm light at 9.93 log quanta deg $^{-2}$ sec $^{-1}$ and 540 nm light at 8.52 log quanta deg $^{-2}$ sec $^{-1}$. The chromaticity co-ordinates of the adapting point are [.703,.296,.001] , approximately equivalent to 630 nm. The axes measure the percent contrast of each component of the signal. The smooth curve sketches the maximum likelihood isodetection contour at 81% correct estimated from the model described later in the text.

Figure 4. The three panels represent Gaussian data from three more observers. The conditions are the same as figure 3 .

Figure 5. Sensitivity to a 6Hz Gabor test stimulus (open circles) compared with the data in figure 3 (filled triangles). Adapting conditions are as in figure 3 .

Figure 6. The three panels plot data for several observers using a 6Hz Gabor function. Adapting conditions as in figure 3 .

Figure 7. Estimated relative spectral sensitivities of two visual channels using the Gaussian timecourse for all observers. The sensitivity is calculated from the detection contours shown in figures 3 and 4.

Figure 8. Spectral sensitivity of the two channels using the 6Hz Gabor function. The data are averaged across three of the observers (open symbols) for one of the channels and across all four observers (filled symbols) for the other. The data from bw corresponding to the open symbols were quite different and are shown separately.

Figure 9. Channel spectral sensitivity estimates from observer bw using the 6Hz Gabor test. The primary channel (open symbols) coincides well with the data from the other observers. The secondary channel is qualitatively different, showing marked opponent sensitivity. This channel has the same spectral opponency as the opponent channel estimated from all observers using the Gaussian test.

Figure 10. Graphic illustration of the predictions of vector difference hypothesis concerning the discriminability of two points, labeled *a* and *b*, that are small perturbations of the adapting field. The two points are predicted to be different if the vector difference between them (solid vector), when displaced to the origin (dashed vector), extends beyond the detection contour.

Figure 11. Pairs of points at discrimination threshold. One point in each pair, the pedestal, is plotted as an open symbol. This point is fixed by the experimenter. The position of the second light, the pedestal plus increment, is plotted as a filled symbol. This point may fall anywhere along a line at 135 degrees (counter-clockwise) to the horizontal axis, starting at the pedestal. The pedestal points were chosen to fall along a line oriented at 22.5 degrees counter-clockwise to the horizontal axis. The pedestal contrasts extend over a range up to roughly 2.5 times threshold. Adapting conditions as in figure 3 .

Figure 12. Additional discrimination thresholds, following the conventions in figure 11 . The new pedestal directions are at 0 deg (along the horizontal axis) and 45 degrees below the horizontal axis. Adapting conditions as in figure 3 .

Figure 13. Detection contour (open symbols) and several discrimination contours (filled symbols) for Gaussian test stimulus. In panel a the discrimination thresholds for various directions around the pedestal are plotted around the position of their respective pedestals (indicated by an X). In panel b, to permit comparison of the shapes of the discrimination contours the data have been slid so that the pedestals fall at the origin. Adapting conditions as in figure 3 .

Figure 14. As in figure 13 but for a second observer.

Figure 15. Pairs of points at discrimination threshold, using a 6Hz Gabor function. The plotting conventions are as in figure 11 . Each panel represents pedestals at a different direction. Panels: a = 22.5 degrees, b = 45 degrees c = 67.5 degrees. Adapting conditions as in figure 3 .

Figure 16. The filled symbols replot all of the pedestal plus increment data points from figure 15 . The lines indicate the range of values of the pedestals in that figure. The pedestal plus increments fall roughly along a common line despite the very wide range of angles swept out by the pedestals. Adapting conditions as in figure 3 .

Figure 17. Discrimination thresholds for pedestals falling along the 135 degree direction and the incremental vector in the 45 degree direction. The adapting conditions for these data were similar to the previous data (see figure

3) except that a steady blue field at 8.381 log quanta deg $^{-2}$ sec $^{-1}$ was added to the steady background. The chromaticity co-ordinates of the adapting field are off the spectral locus at [.683,.285,.032]. The observer is ac.

Figure 18. A replot of the pedestal plus test data points from figure 17 . The points fall along a common line.

Figure 19. Discrimination thresholds for different directions around a pedestal in the 22.5 degree direction. Adapting field as in figure 17 . Notice that the shapes of the contours are quite different, and that discriminations in the direction away from the pedestal vector strongly violate the vector difference hypothesis. Observer is bw.

Figure 20. Detection contour (open symbols) and discriminations contours (filled symbols) of 6Hz Gabor functions modulated in the iso-luminance plane. The adapting field is described in figure 17 . Stimulus co-ordinates for two of the channels are plotted and the modulation of the third beam (440nm) may be determined from the other two since the combination of modulations must remain within the iso-luminance plane. Although three discrimination contours were measured only two are shown in this figure in order to avoid cluttering the graph. The third is presented in the next figure. Observer is bw.

Figure 21. Iso-luminance detection contour (open symbols) and three discrimination contours (filled symbols). The discrimination contours have been slid so that their pedestals fall on the origin to permit a comparison of the shapes of the discrimination contours and the detection contour. Adapting conditions as in figure 17 . Observer is bw.

Figure 22. Iso-sensitivity lines for two mechanisms, and an iso-detection contour calculated on the assumption of probability summation between the mechanisms. The horizontal axis represents the degree of excitation of one mechanism, and the vertical axis represents the degree of excitation of a second mechanism. Dashed lines parallel to the horizontal and vertical axes represent iso-sensitivity lines of the two mechanisms. The dark, dashed circle is the iso-detection contour for probability summation between the two mechanisms. See text for further details.

References

Boynton, R. M., Ikeda, M., & Stiles, W. S. (1964) Interactions among chromatic mechanisms as inferred from positive and negative increment thresholds. *Vision Res.* **4** ,87-117

Brown, W. R. J. (1951) The influence of luminance level on visual sensitivity to color differences. *J. Opt. Soc. Am.* **41**(10),684-688

Brown, W. R. J. (1952) Statistics of color-matching data. *J. Opt. Soc. Am.* **42**(4),252-256

Campbell, F. W. & Robson, J. G. (1968) Application of Fourier analysis to the visibility of gratings. *J. Physiol., Lond.* **197** ,551-566

Gabor, D. (1946) Theory of Communication. *J.IEE London,* **93**(III),429-457

Green, D. M. & Luce, R. D. (1975) Parallel psychometric functions from a set of independent detectors. *Psychol. Rev.* **82** ,483-486

Guth, S. L., Donley, N. J., & Marrocco, R. T. (1969) On luminance additivity and related topics. *Vision Res.* **9**,537-575

Horn, B. K. P. (1974) Determining lightness from an image. *Computer Graphics and Image Processing* **3**,277-299

Hurvich, L. M. & Jameson, D. (1955) Some quantitative aspects of an opponent-colors theory. II. Brightness, saturation and hue in normal and dichromatic vision. *Journal of the Optical Society of America* **45**,602-616

Kelly, D. H. & Norren, D. van (1977) Two-band model of heterochromatic flicker. *J. Opt. Soc. Amer.* **67** ,1081-1091

Kirk, D. B. (1982) Color discrimination at threshold: the approach through increment threshold sensitivity. *Vision Res.* **22**(7),713-720

Kranda, K. & King-Smith, P. E. (1979) Detection of coloured stimuli by independent linear systems. *Vision Res.* **19** ,733-746

Larimer, J. (1981) Red/green opponent colors equilibria measured on chromatic adapting fields: evidence for gain changes and restoring forces. *Vision Res.* **21**,501-512

Larimer, J., Krantz, D. H., & Cicerone, C. M. (1974) Opponent-process additivity -- I. Red/green equilibria. *Vision Res.* **14**,1127-1140

MacAdam, D. L. (1942) Visual sensitivities to color differences in daylight. *Journal of the Optical Society of America* **32**,247-274

MacAdam, D. L. (1943) Specification of small chromaticity differences. *J. Opt. Soc. Am.* **33**,18

Maloney, L. T. & Wandell, B. A. (1983) The slope of the psychometric functions at different wavelengths. *Supplement to Investigative Opthalmology and Visual Science* **24**(3),183A

Maloney, L. T. & Wandell, B. A. (1984) A model of a single visual channel's response to weak test lights. *Vision Res.* **in press.**,

Quick, R. F. (1974) A vector magnitude model of contrast detection. *Kybernetik* **16**,65-67

Rosen, P., Levine, M. W., Rosetto, M., & Abramov, I. (1970) A system for controlling the light output of a monochromator by any simple function and for temporally modulating intensity.. *Behav. Res. Meth. & Instru.* **2**(6),297-300

Sagi, D. & Hochstein, S. (1983) Discriminability of suprathreshold compound spatial frequency gratings. *Vision Res.* **23**(12),1595-1608

Silberstein, L. & MacAdam, D. L. (1945) The distribution fo color matchings around a color center. *J. Opt. Soc. Am.* **35**(1),32-39

Stiles, W. S. (1967) Mechanism concepts in colour theory. *J. of the Colour Group* (11),106-123

Thornton, J. & Jr., E. N. Pugh (1983) Red/green color opponency at detection threshold. *Science* **219**,191-193

Wandell, B. A. (1982) Measurements of small color differences. *Psych. Rev.* **89**,281-302

Wandell, B. A. & Luce, R. D. (1978) Pooling peripheral information: averages versus extreme values. *J. Math. Psych.* **17**(3),220-234

Wandell, B. A. & Pugh, E. N. (1980) Detection of long-duration, long-wavelength incremental flashes by a chromatically coded pathway. *Vision Res.* **20** ,625-636

Wandell, B. A., Sanchez, J., & Quinn, B. (1982) Detection/discrimination in the long-wavelength pathways. *Vision Res.* **22**(8),196-201

Watson, A. B. (1979) Probability summation over time. *Vision Res.* **19** ,515-522

Watson, A. B. (1984) Detection and recognition of simple spatial forms. *NASA TM* **84353**,

Wilson, H. R. & Gelb, D. J. (1984) Modified line-element theory for spatial-frequency and width discrimination. *J. Opt. Soc. Am.* **1**(1),124-131

Wyszecki, G. & Stiles, W. S. (1967) *Color Science.* John Wiley and Sons, New York.

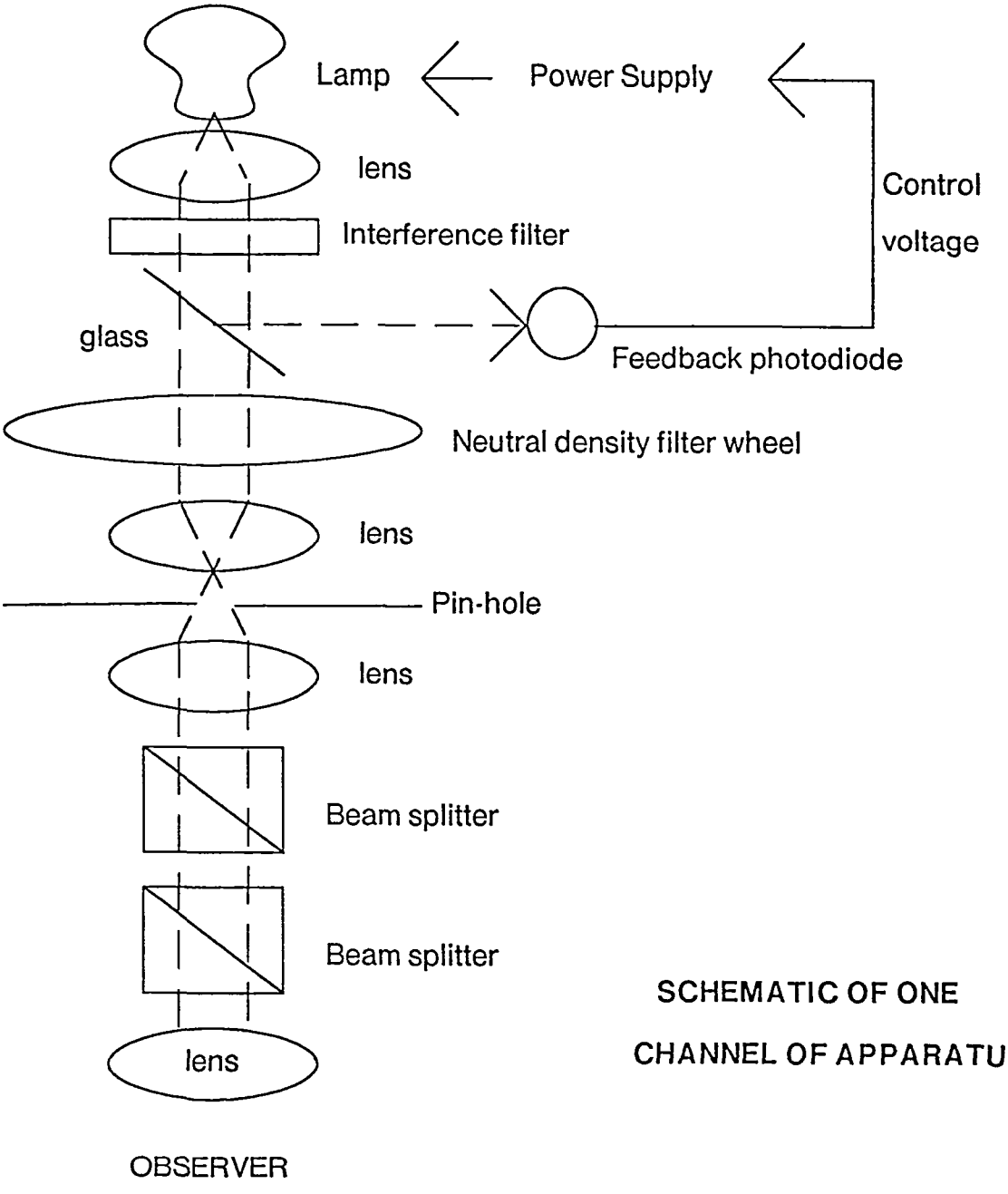

SCHEMATIC OF ONE CHANNEL OF APPARATUS

FIGURE 1

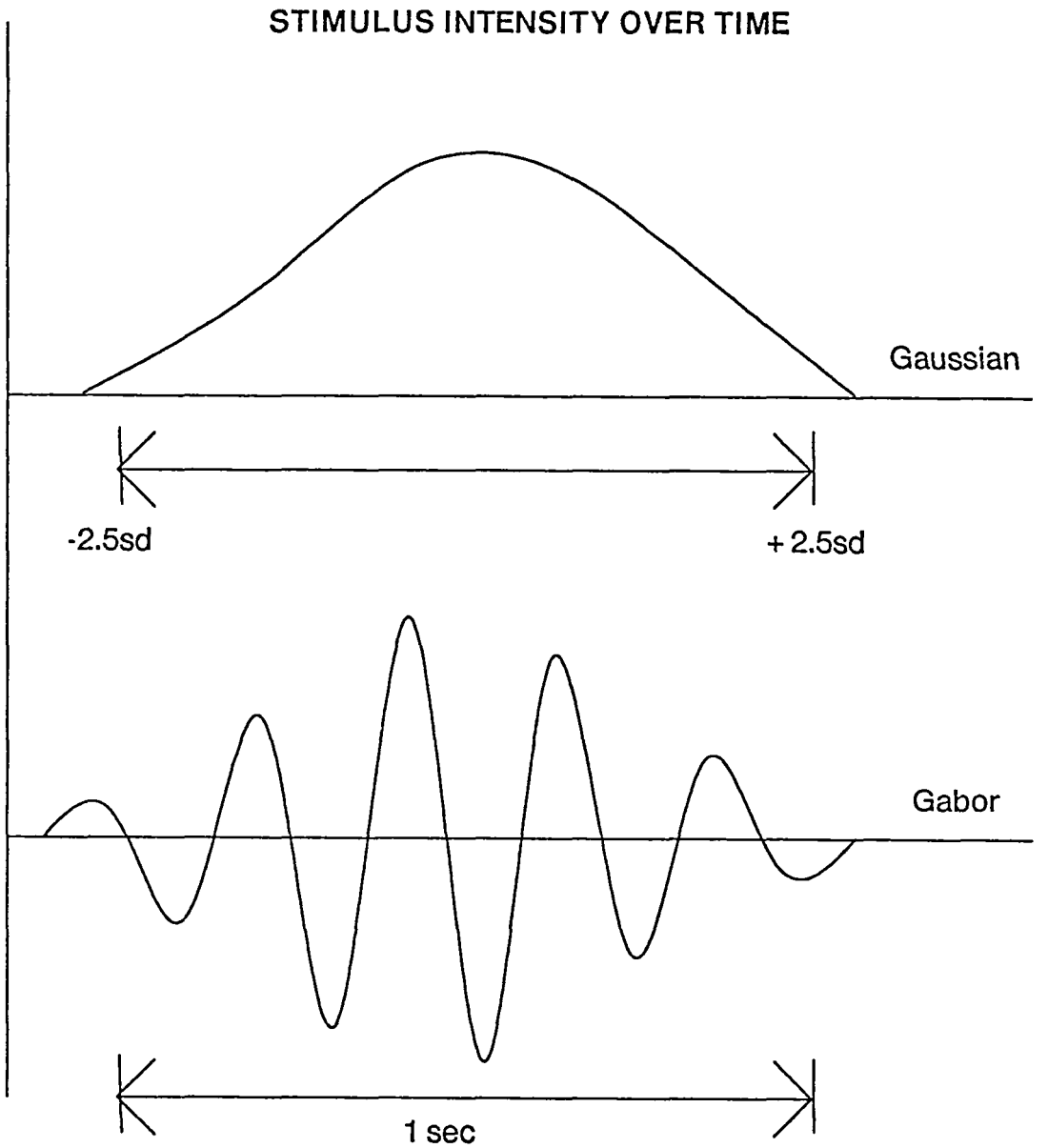
STIMULUS INTENSITY OVER TIME
Gaussian
-2.5sd
+2.5sd
Gabor
1 sec

FIGURE 2

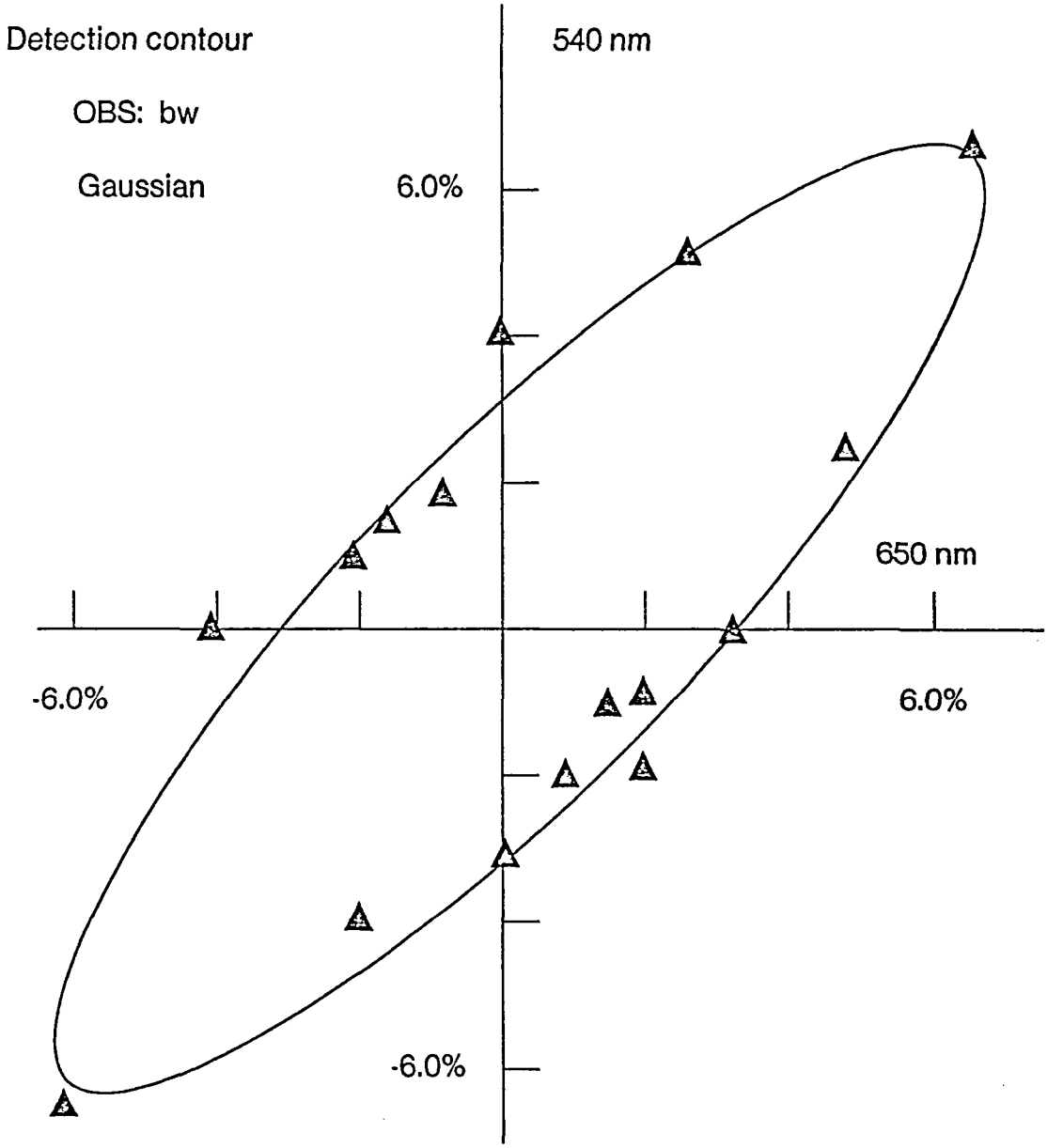

FIGURE 3

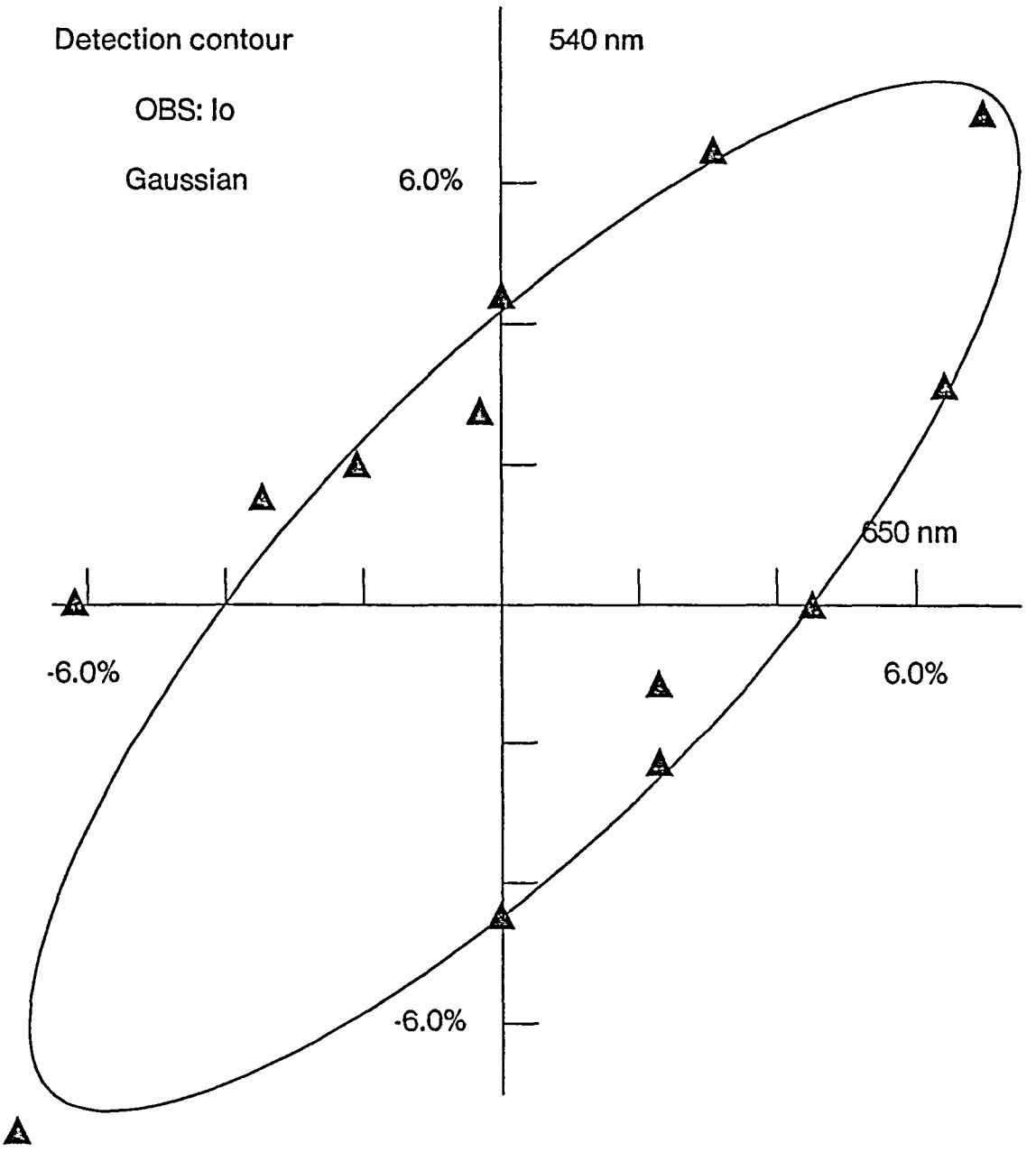

FIGURE 4a

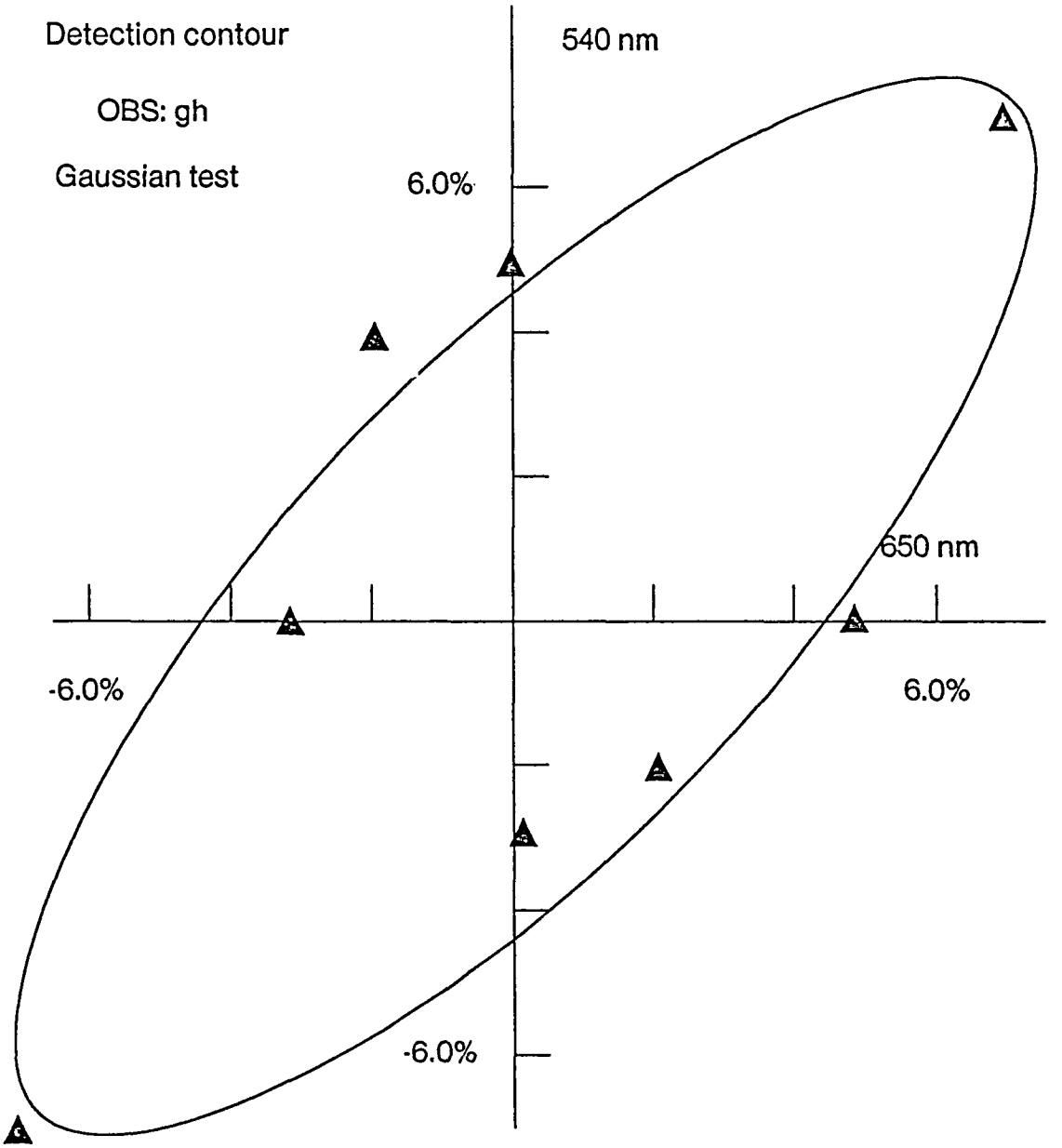
Detection contour
OBS: gh
Gaussian test
540 nm
6.0%
650 nm
-6.0%
6.0%
-6.0%

FIGURE 4b

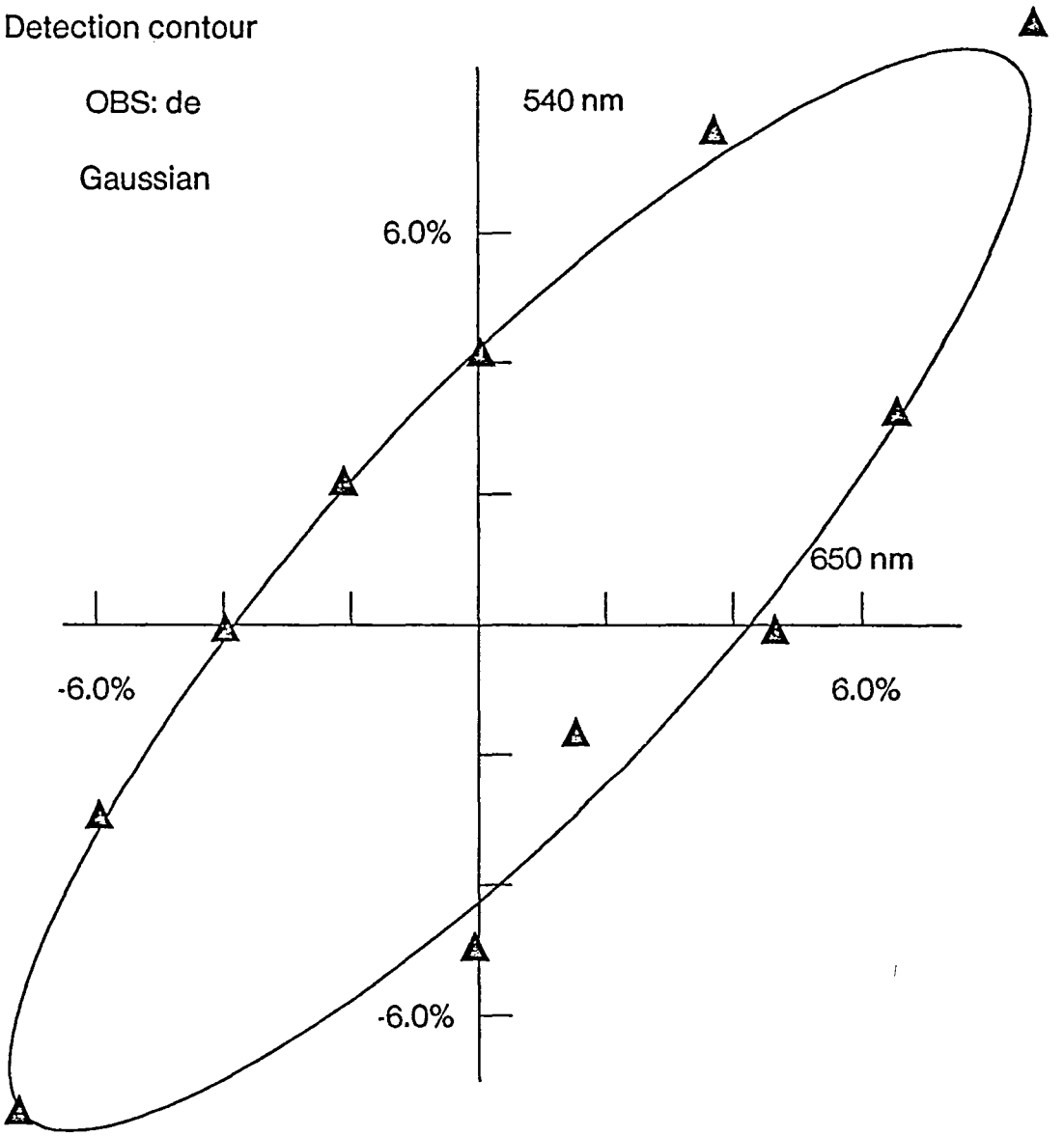

FIGURE 4c

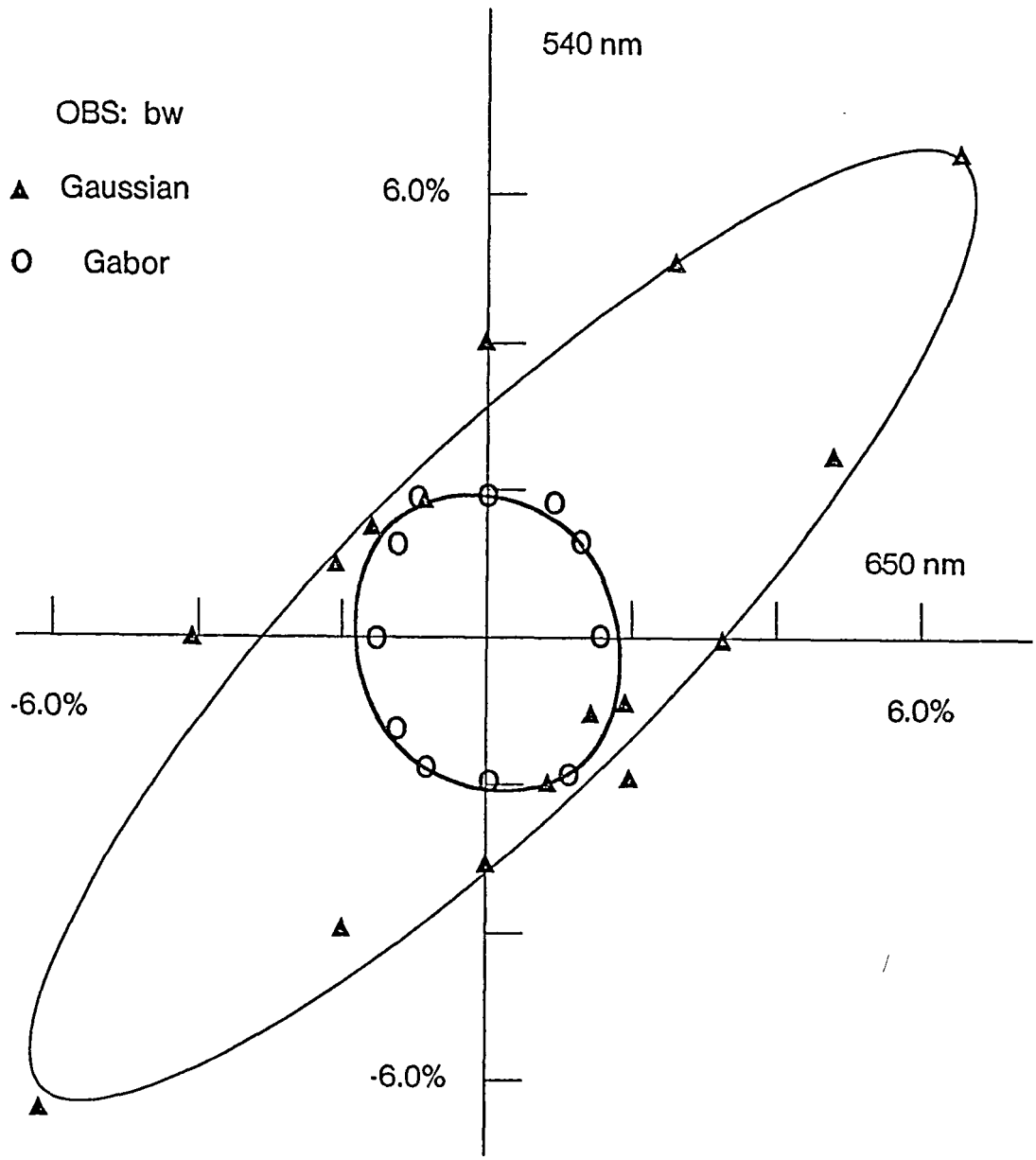

FIGURE 5

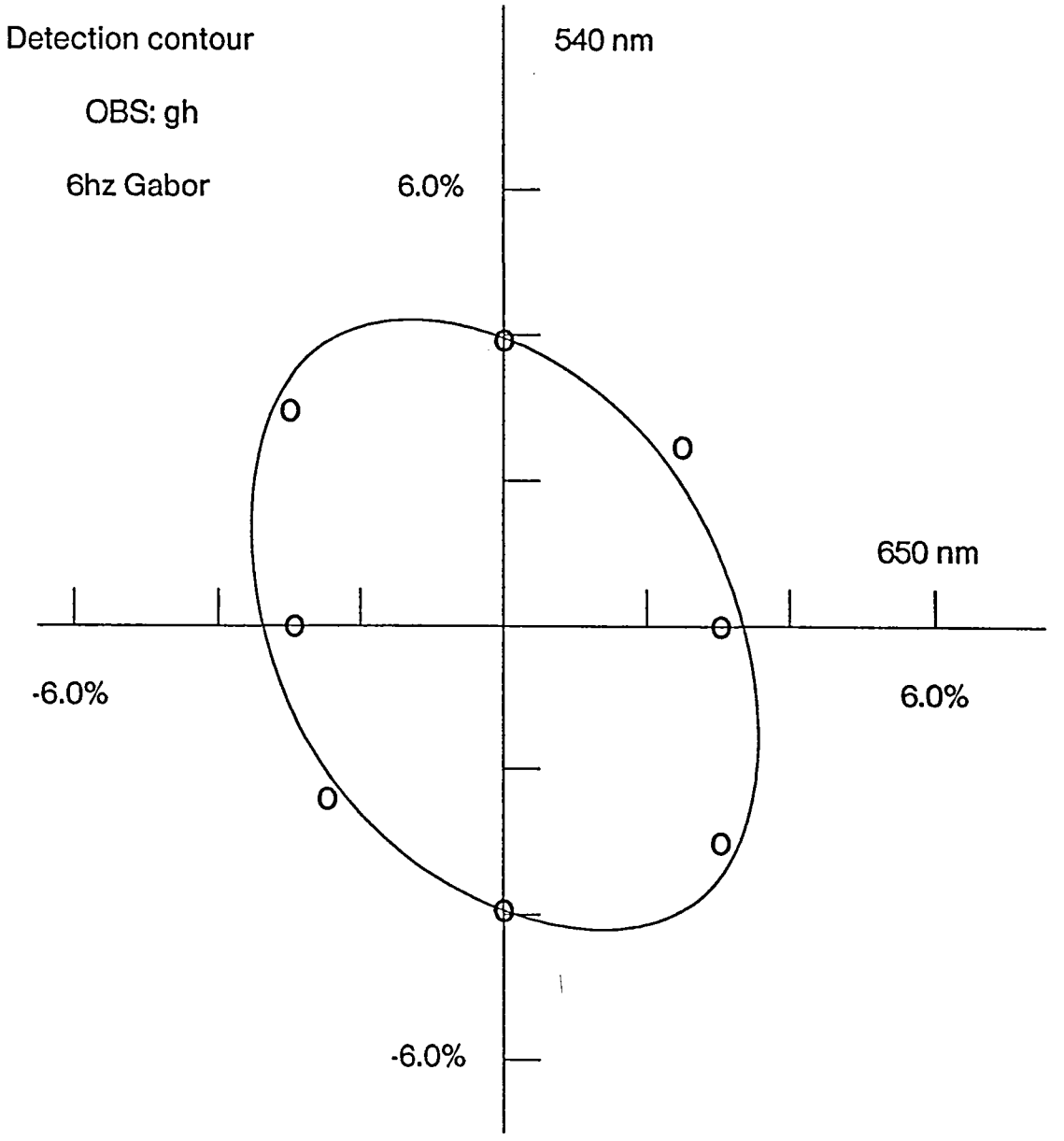

FIGURE 6a

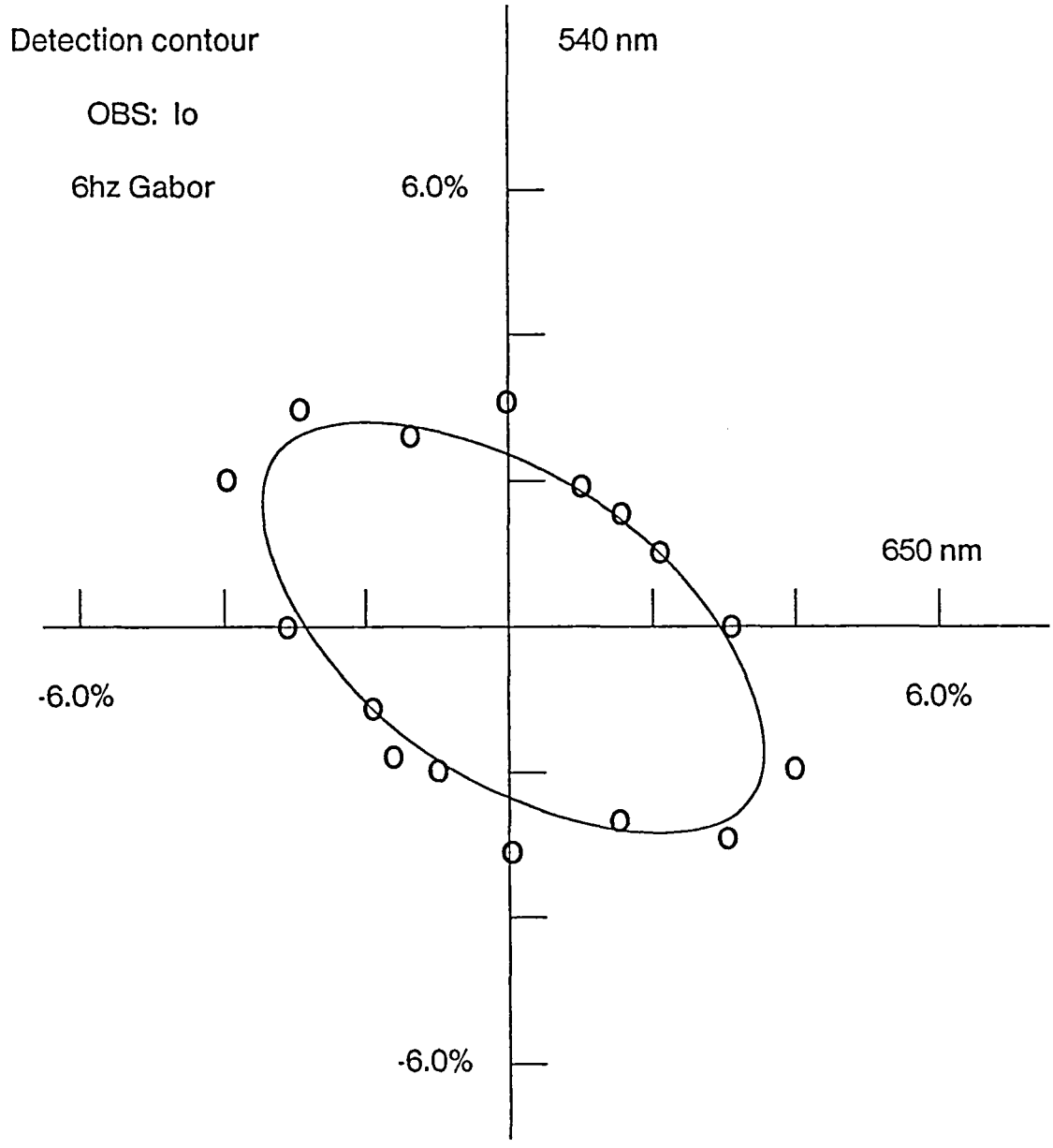

FIGURE 6b

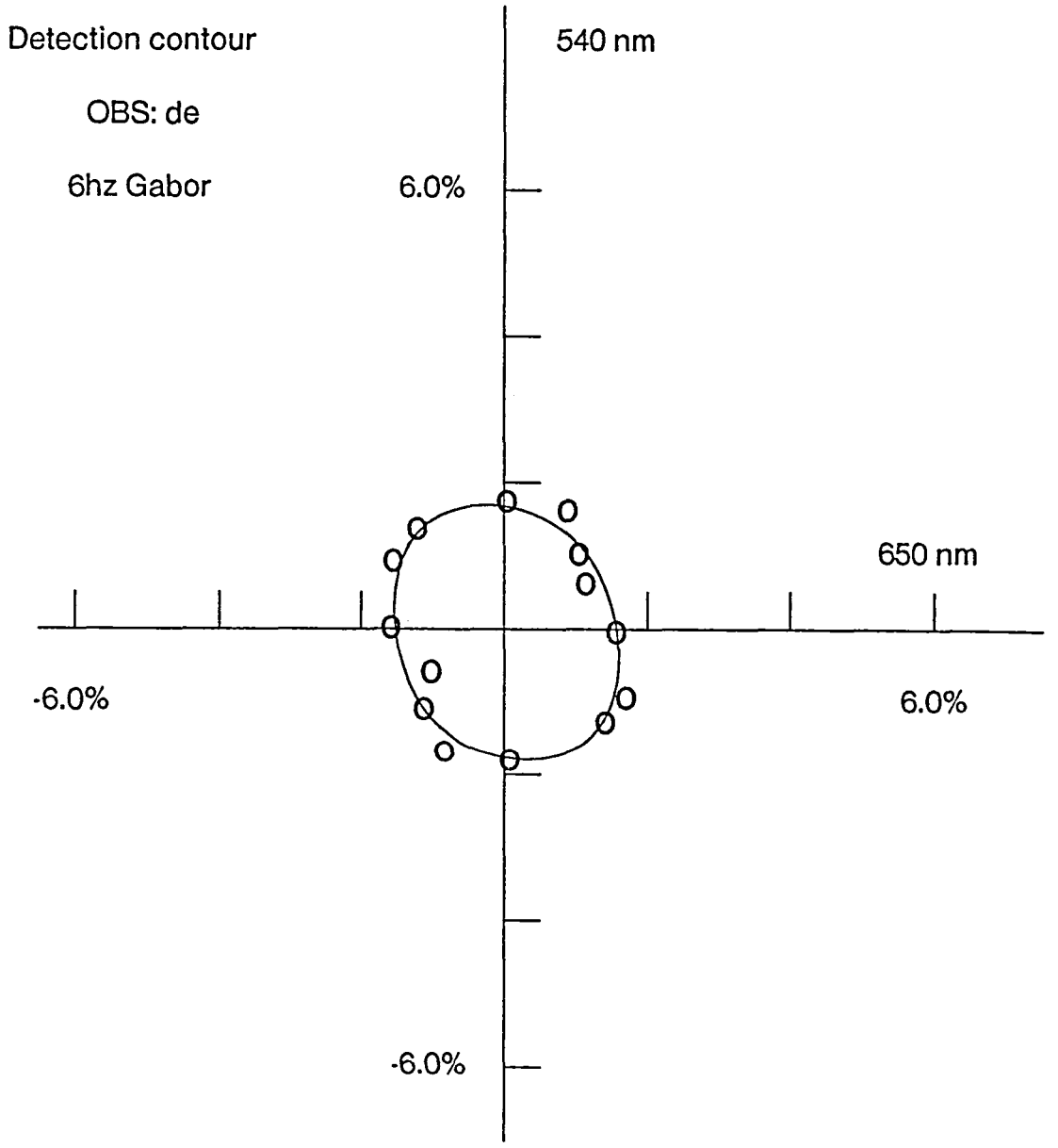

FIGURE 6c

CIRCULAR ISO-DETECTION CONTOUR
DRAWN IN MECHANISM CO-ORDINATES

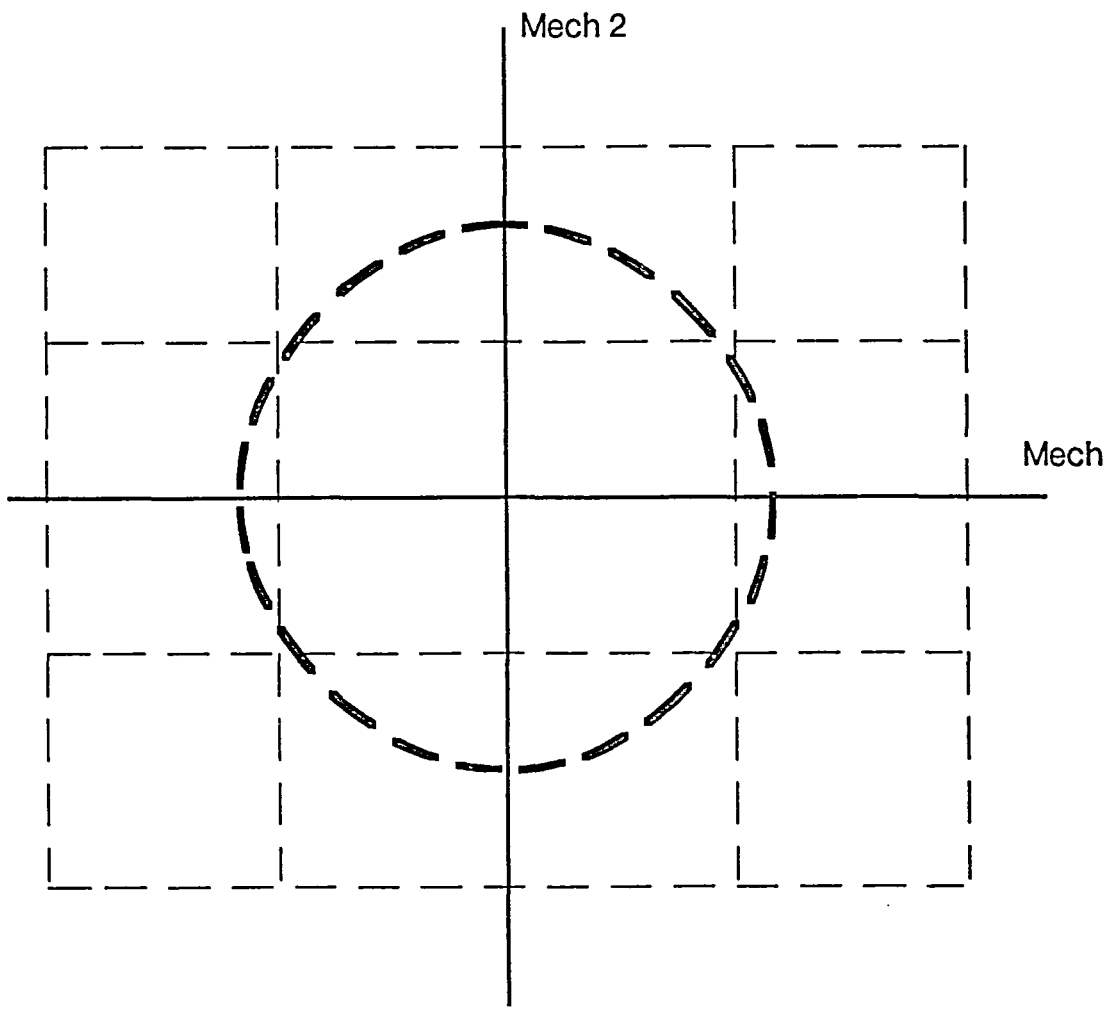

Vertical dashed lines are iso-response lines of mech 1

Horizontal dashed lines are iso-response lines of mech 2

FIGURE 7

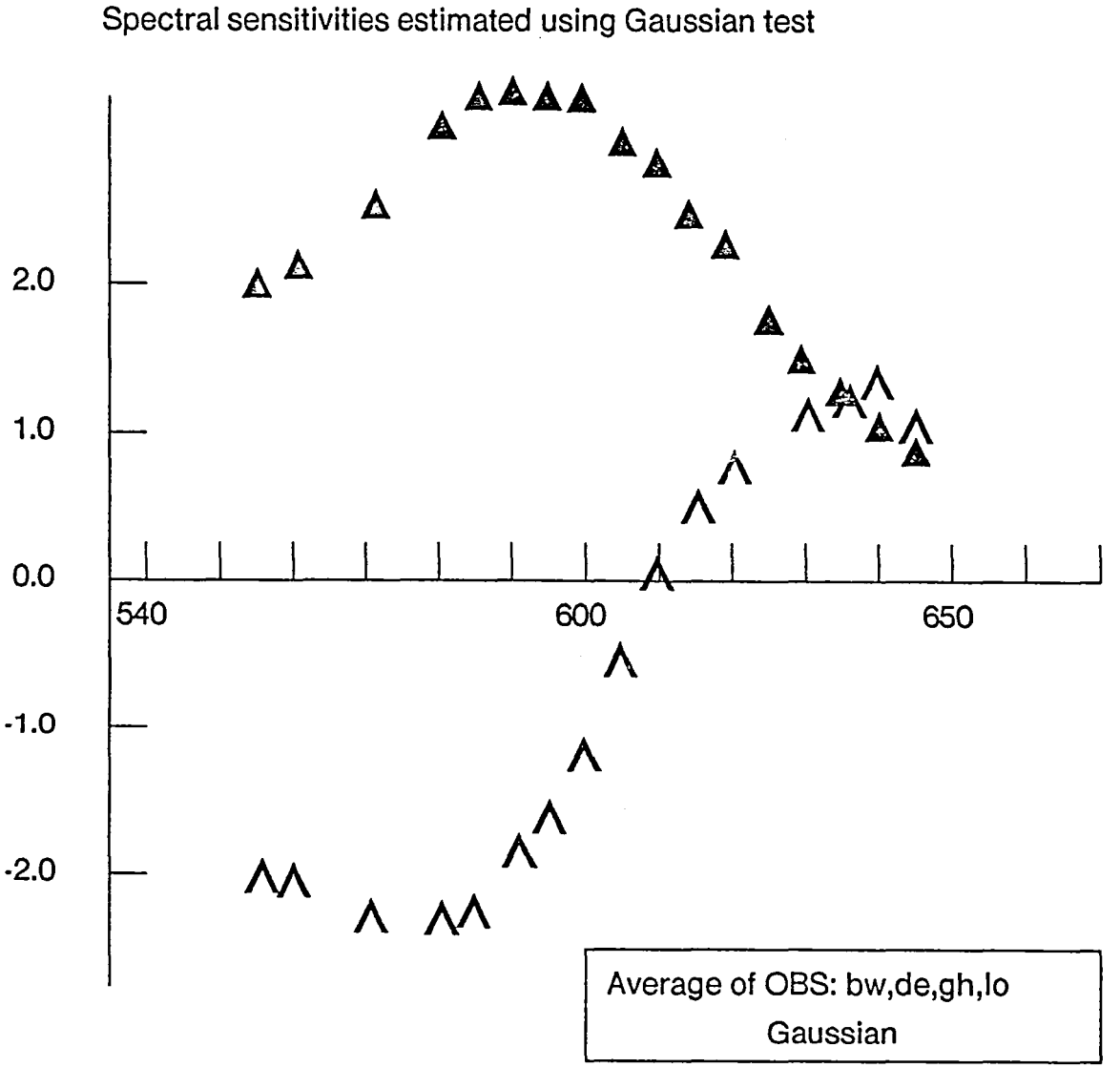
Spectral sensitivities estimated using Gaussian test
2.0
1.0
0.0
-1.0
-2.0
540
600
650
Average of OBS: bw,de,gh,lo
Gaussian

FIGURE 8

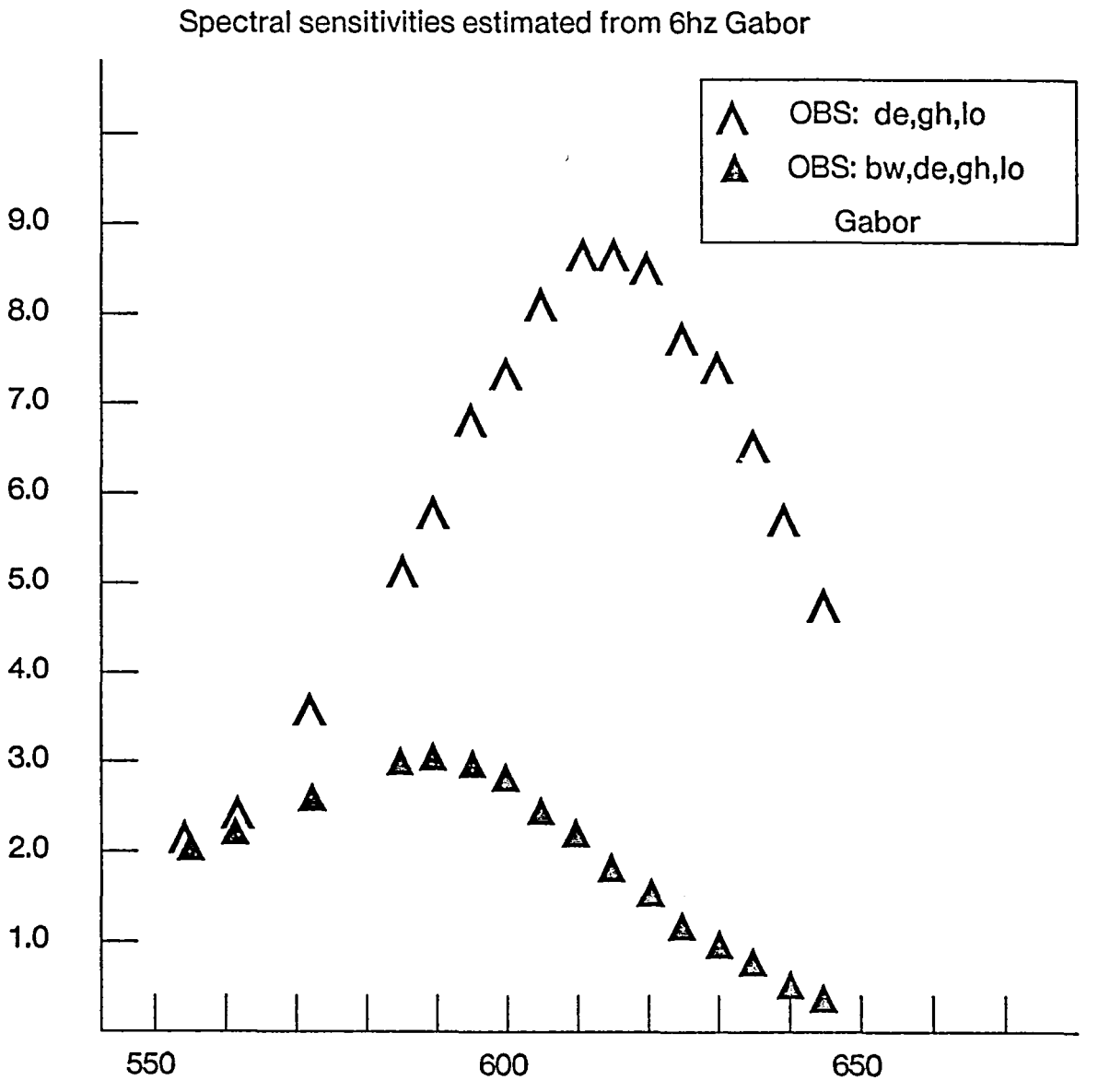
Spectral sensitivities estimated from 6hz Gabor
OBS: de,gh,lo
OBS: bw,de,gh,lo
Gabor
9.0
8.0
7.0
6.0
5.0
4.0
3.0
2.0
1.0
550
600
650

FIGURE 9

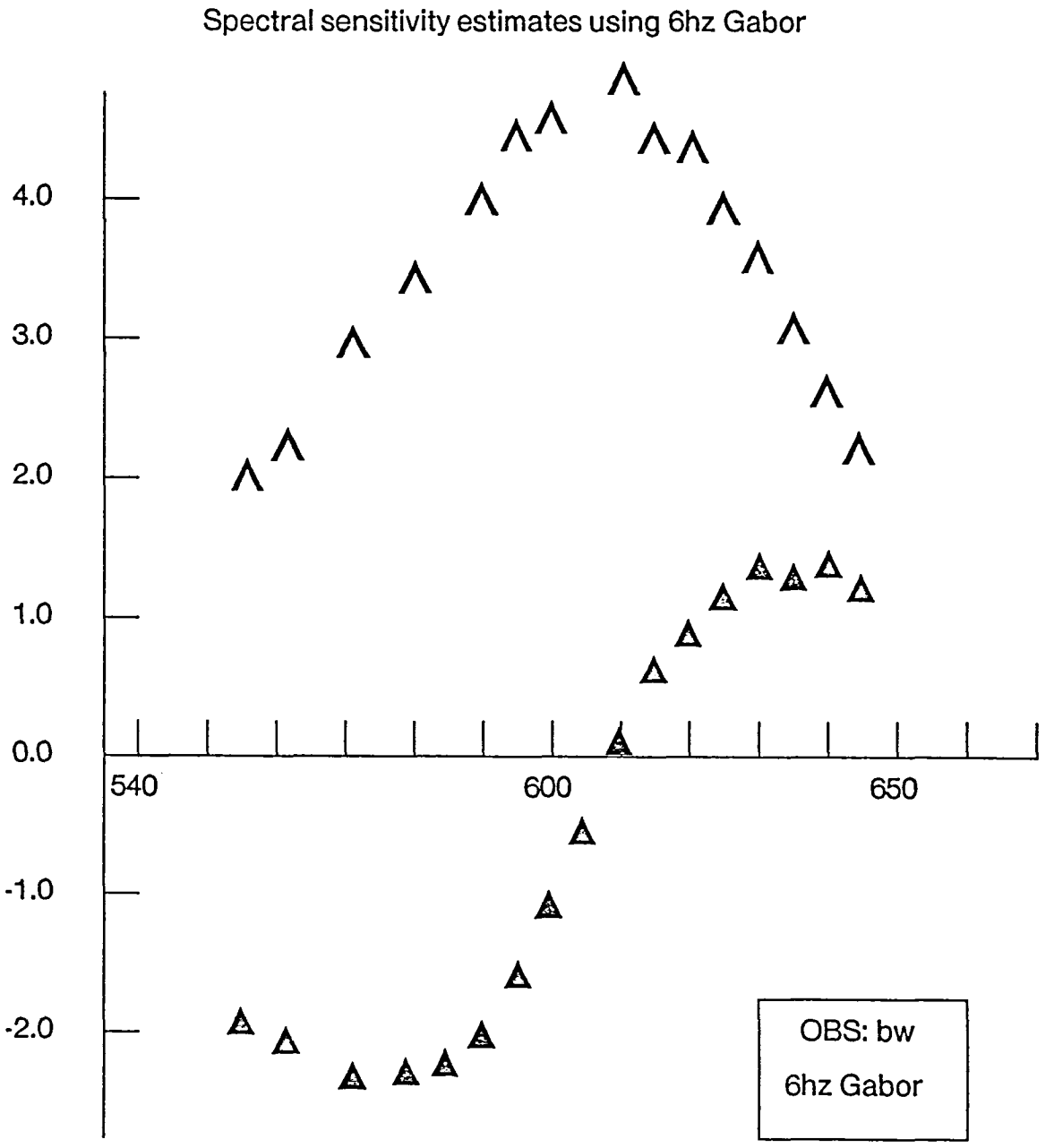
Spectral sensitivity estimates using 6hz Gabor
4.0
3.0
2.0
1.0
0.0
-1.0
-2.0
540
600
650
OBS: bw
6hz Gabor

FIGURE 10

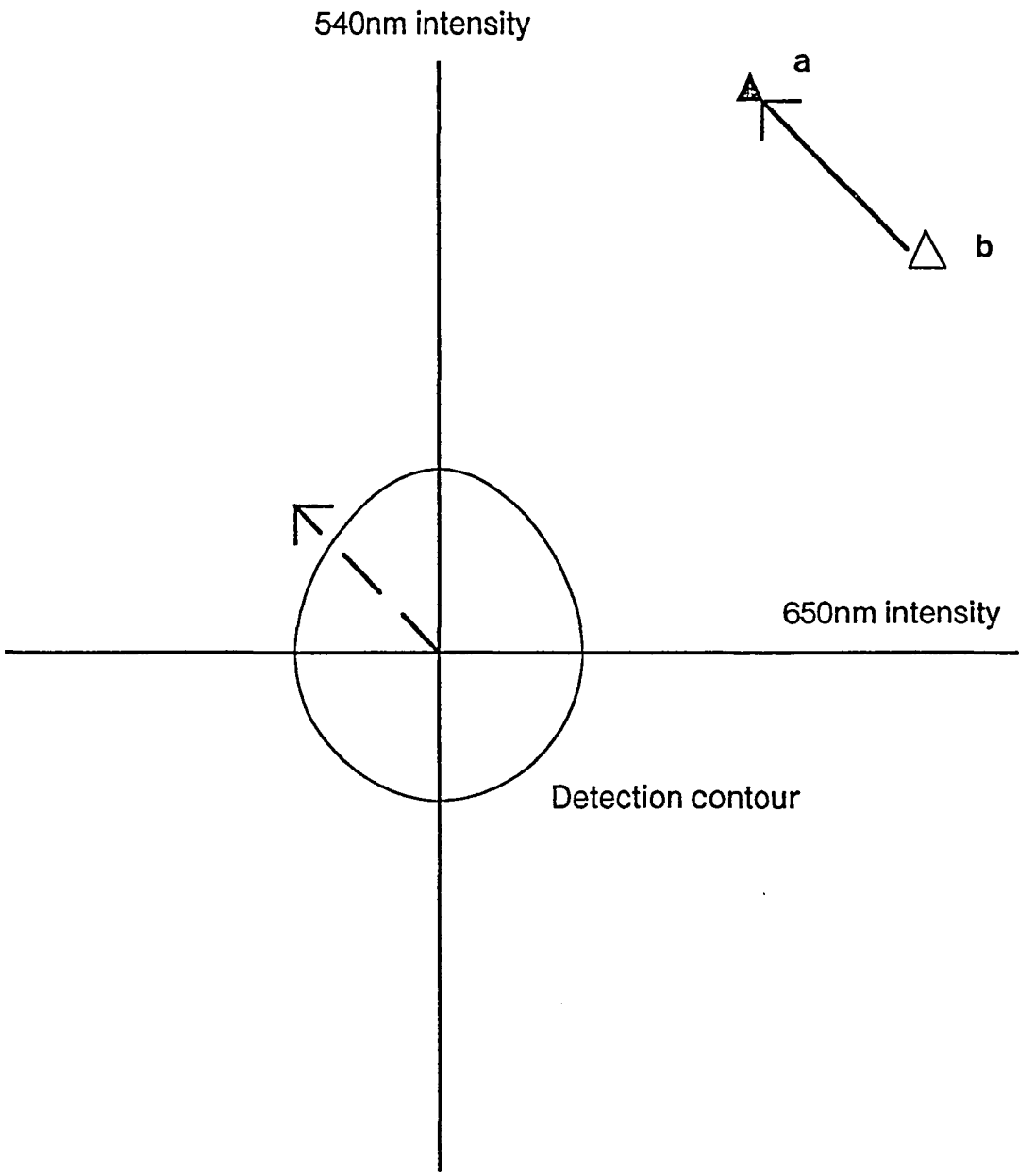

FIGURE 11

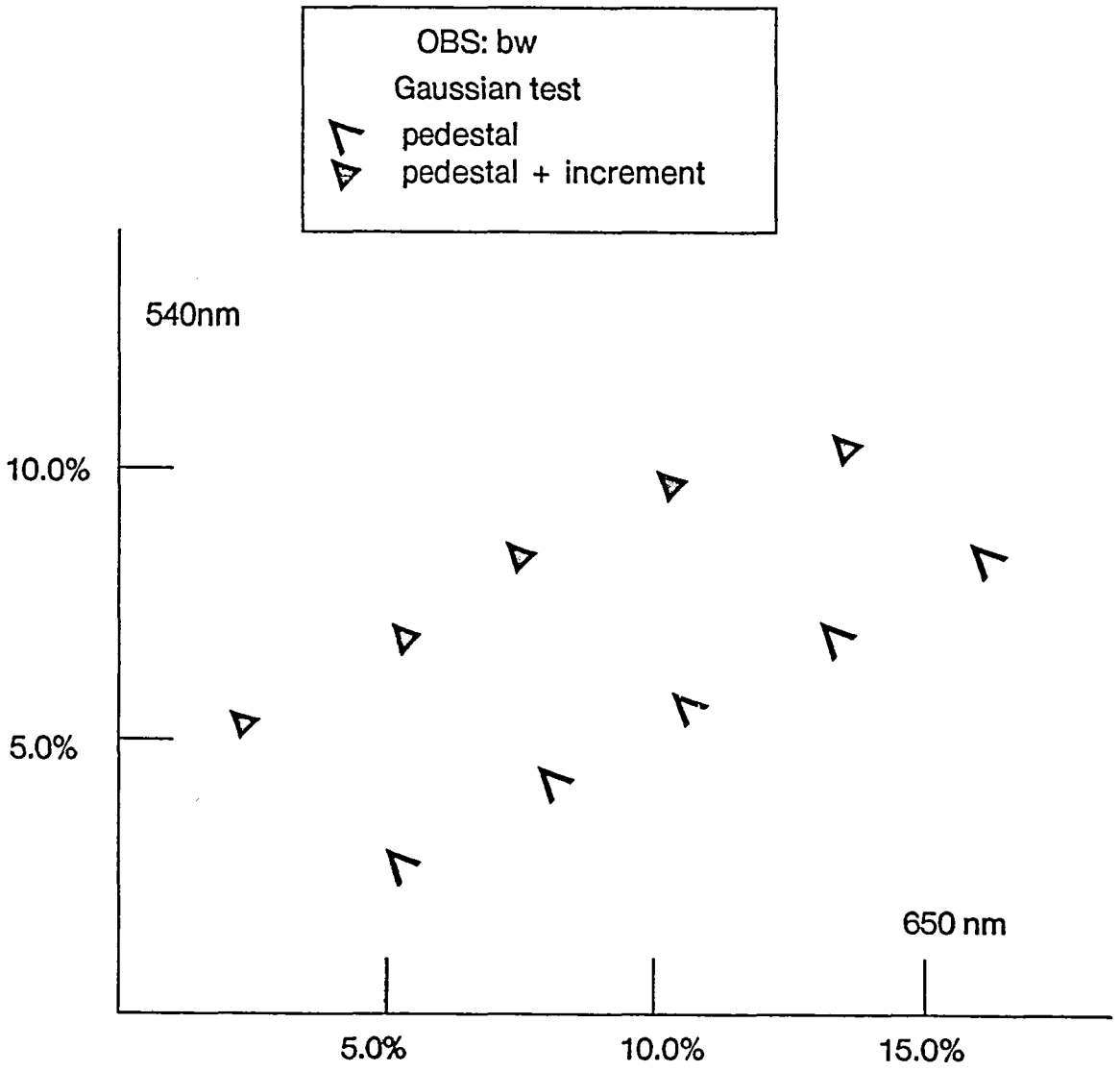
OBS: bw
Gaussian test
pedestal
pedestal + increment
540nm
10.0%
5.0%
650 nm
5.0%
10.0%
15.0%

FIGURE 12

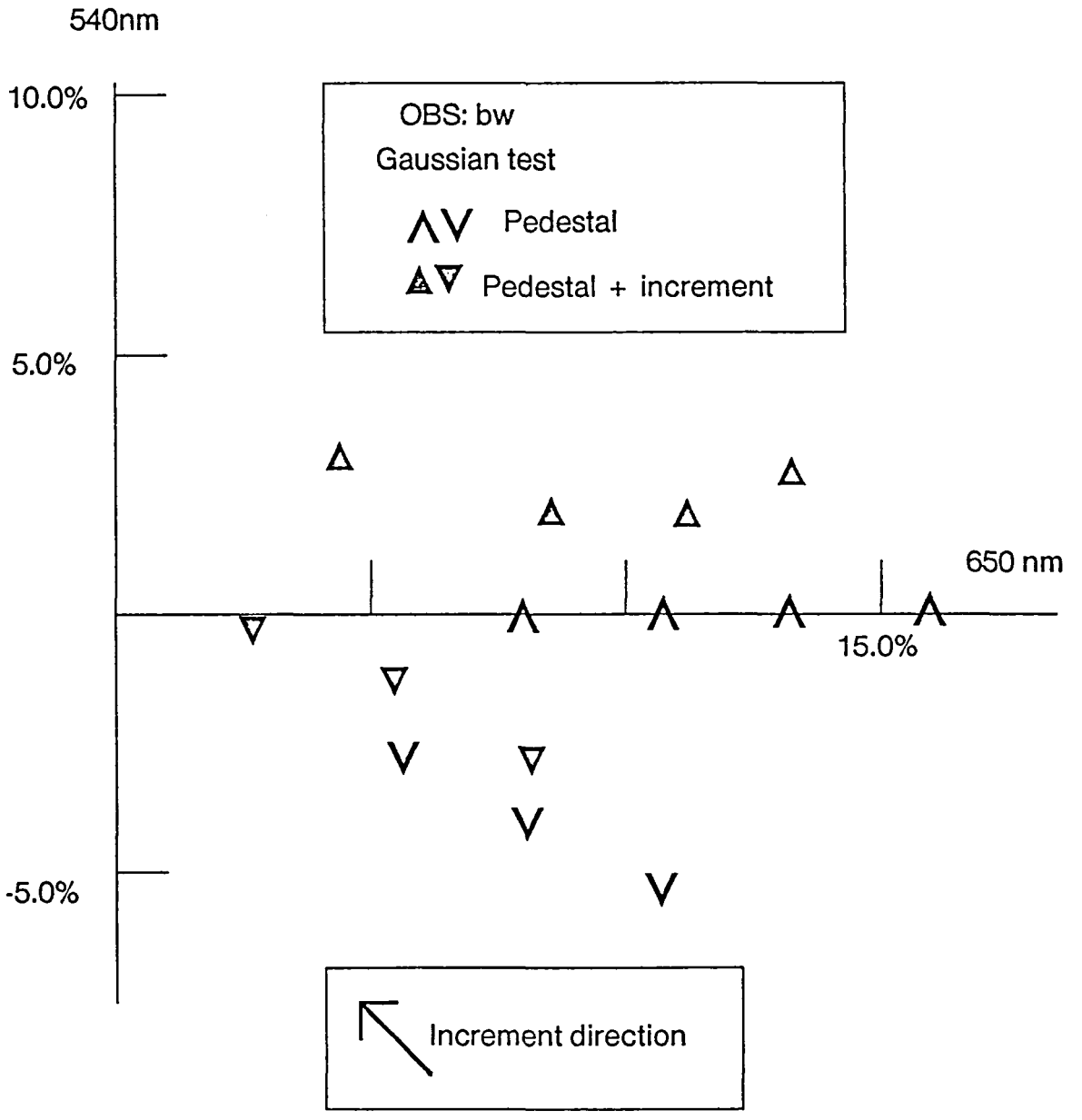
540nm
10.0%
5.0%
-5.0%
OBS: bw
Gaussian test
Pedestal
Pedestal + increment
650 nm
15.0%
Increment direction

FIGURE 13

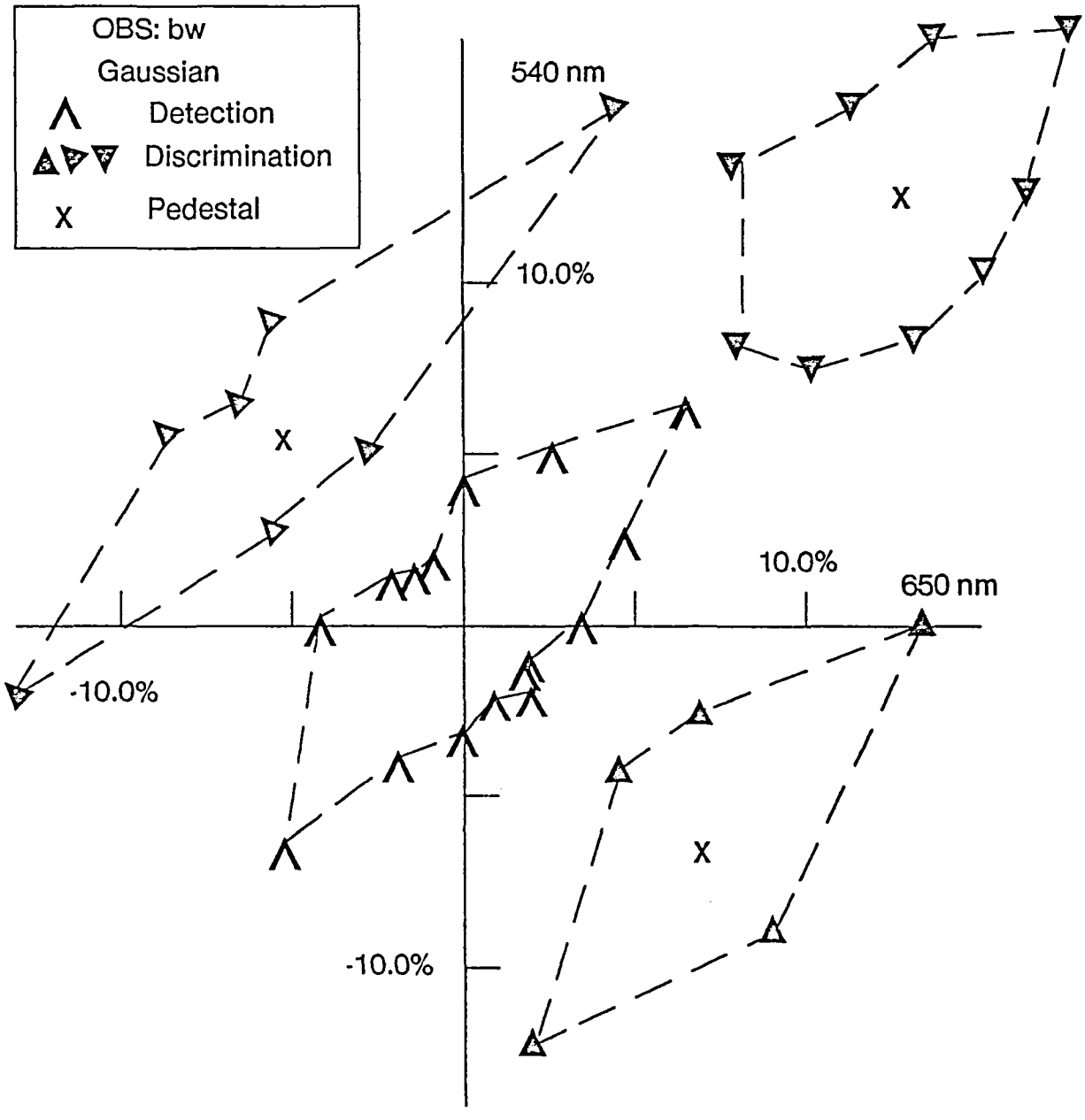
OBS: bw
Gaussian
Detection
Discrimination
Pedestal
540 nm
10.0%
10.0%
650 nm
-10.0%
-10.0%
X
X
X

FIGURE 14a

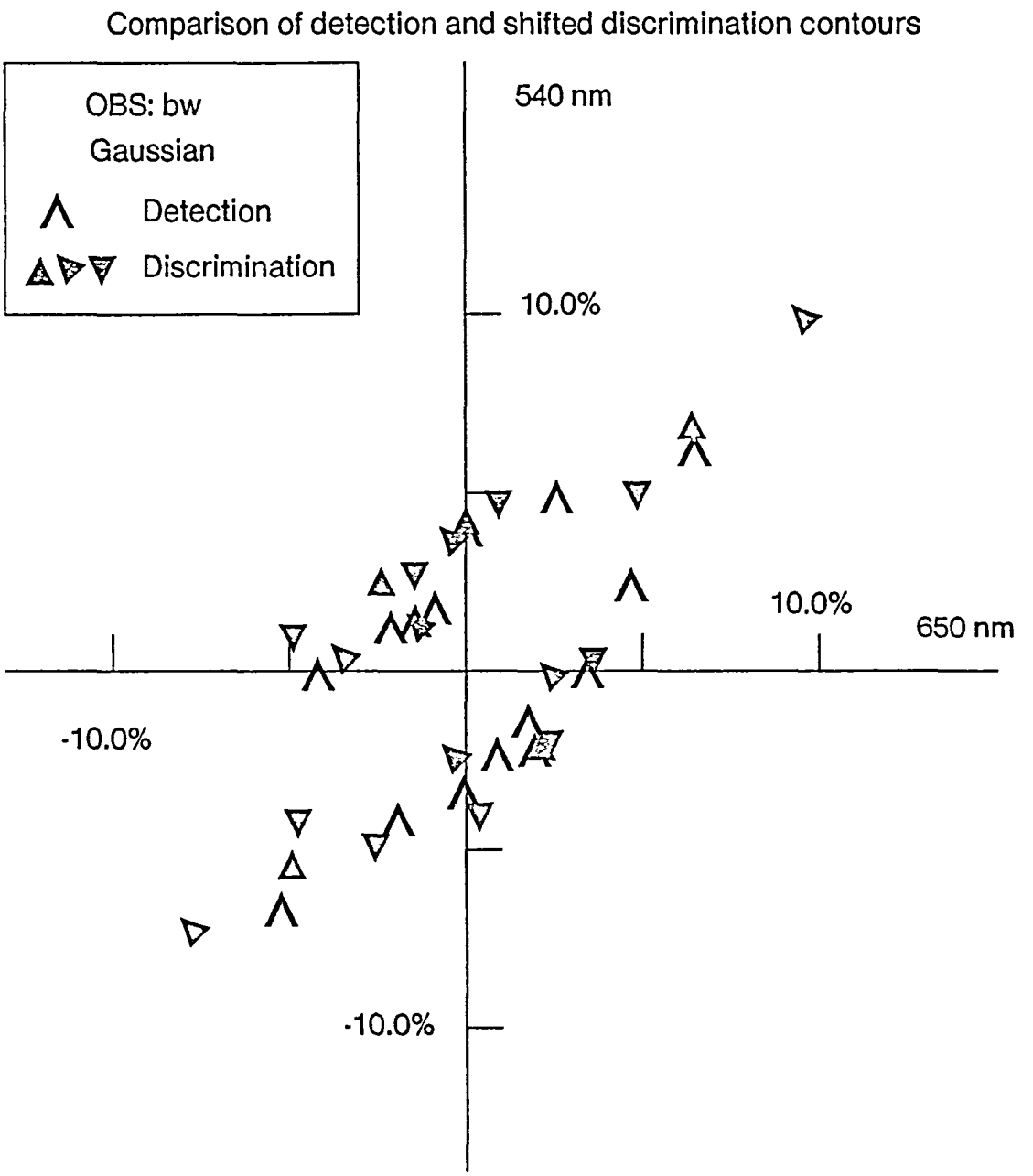
Comparison of detection and shifted discrimination contours
OBS: bw
Gaussian
Detection
Discrimination
540 nm
10.0%
10.0%
650 nm
-10.0%
-10.0%

FIGURE 14b

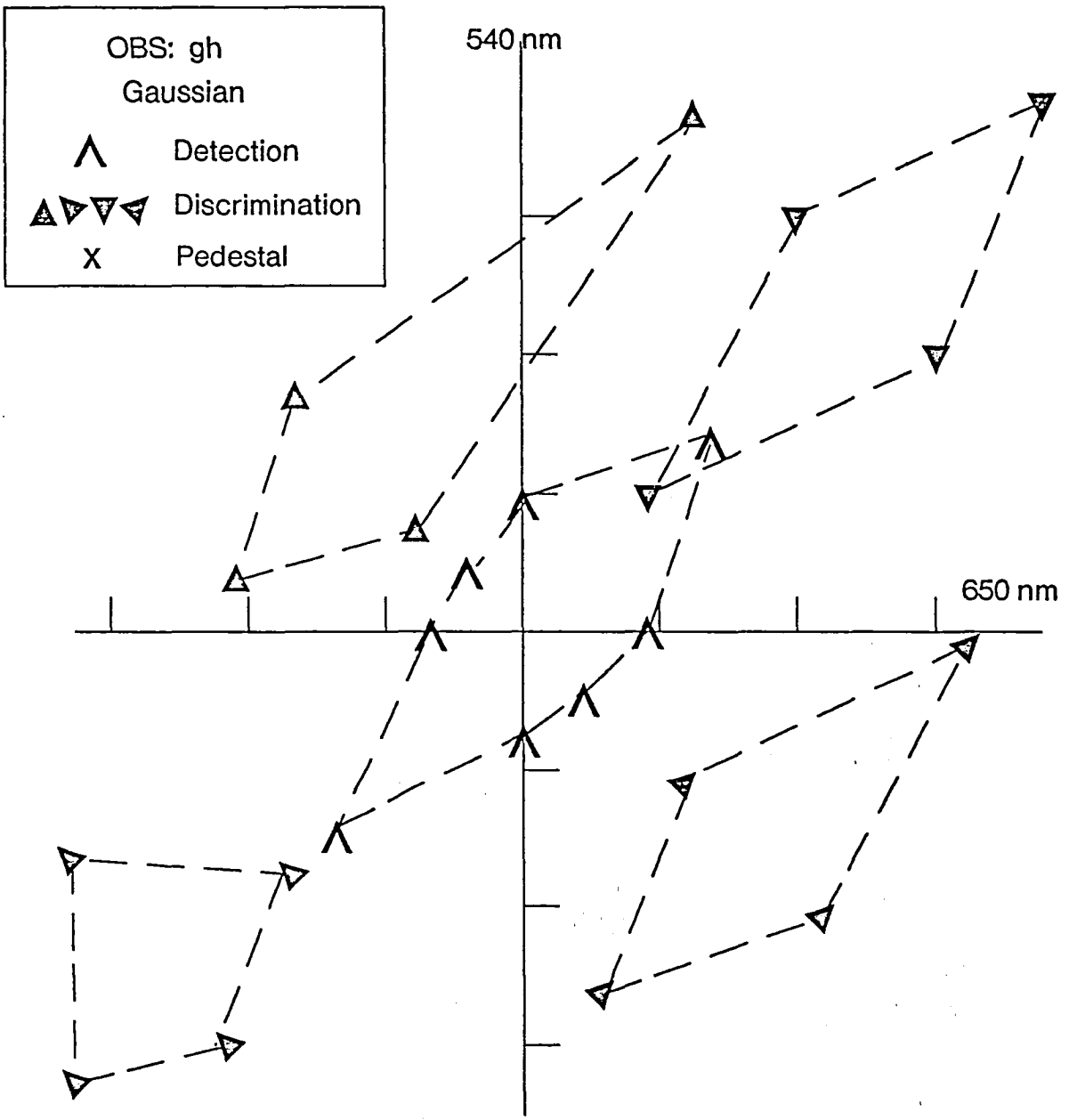
OBS: gh
Gaussian
Detection
Discrimination
Pedestal
540 nm
650 nm

FIGURE 15a

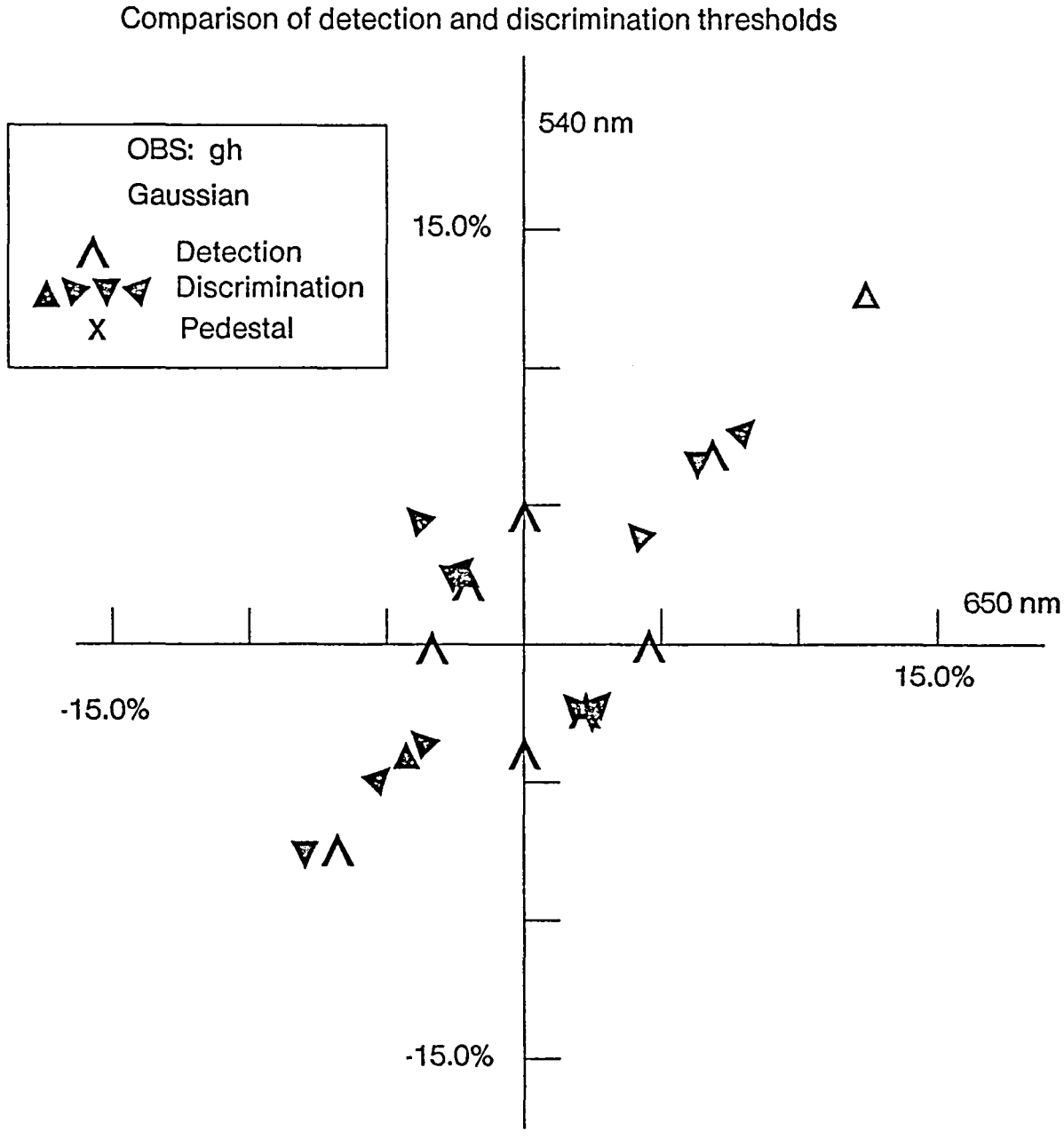
Comparison of detection and discrimination thresholds
OBS: gh
Gaussian
Detection
Discrimination
Pedestal
540 nm
15.0%
650 nm
15.0%
-15.0%
-15.0%

FIGURE 15b

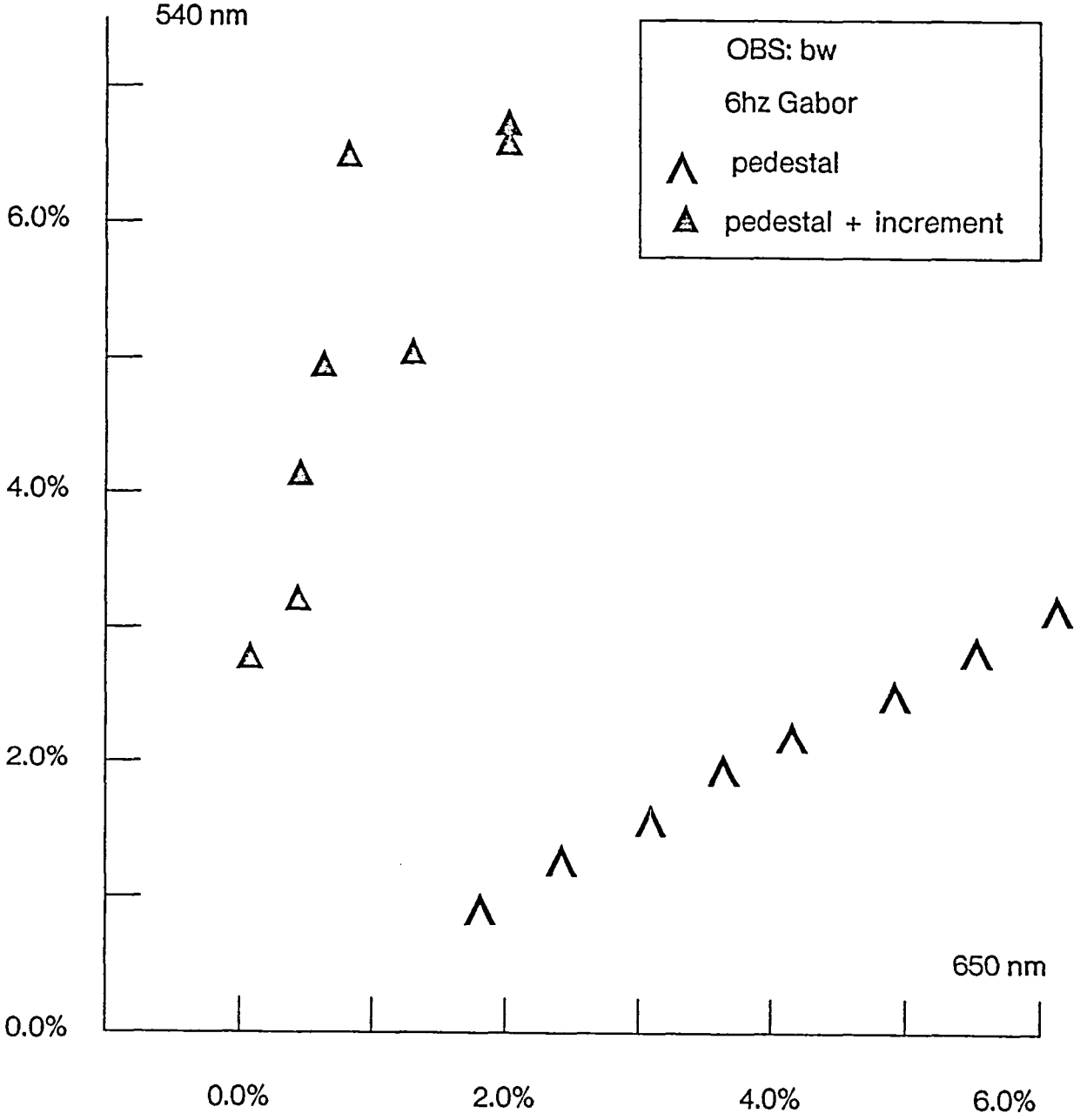
540 nm
OBS: bw
6hz Gabor
pedestal
pedestal + increment
6.0%
4.0%
2.0%
0.0%
650 nm
0.0%
2.0%
4.0%
6.0%

FIGURE 16a

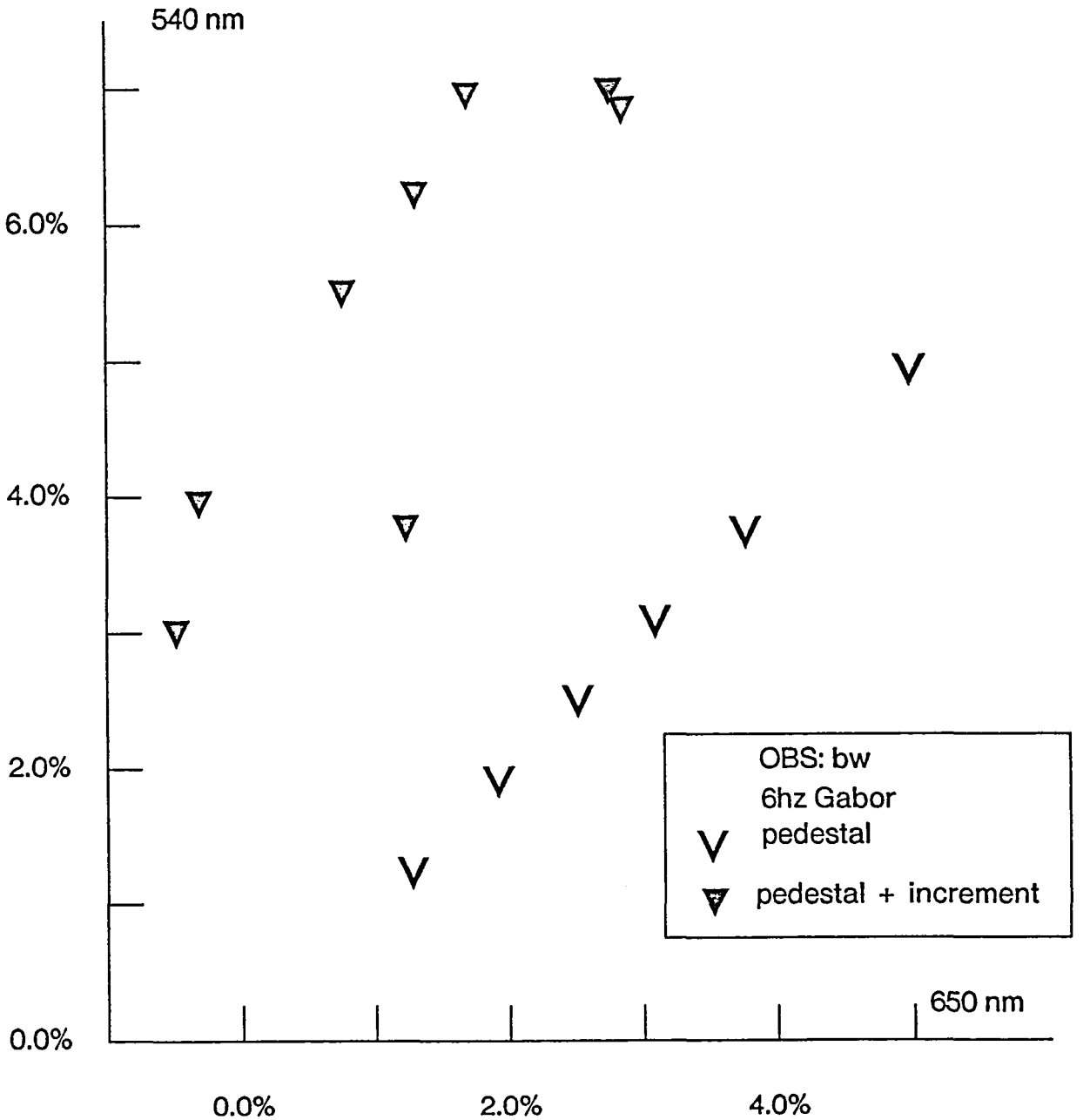
540 nm
6.0%
4.0%
2.0%
0.0%
650 nm
0.0%
2.0%
4.0%
OBS: bw
6hz Gabor
pedestal
pedestal + increment

FIGURE 16b

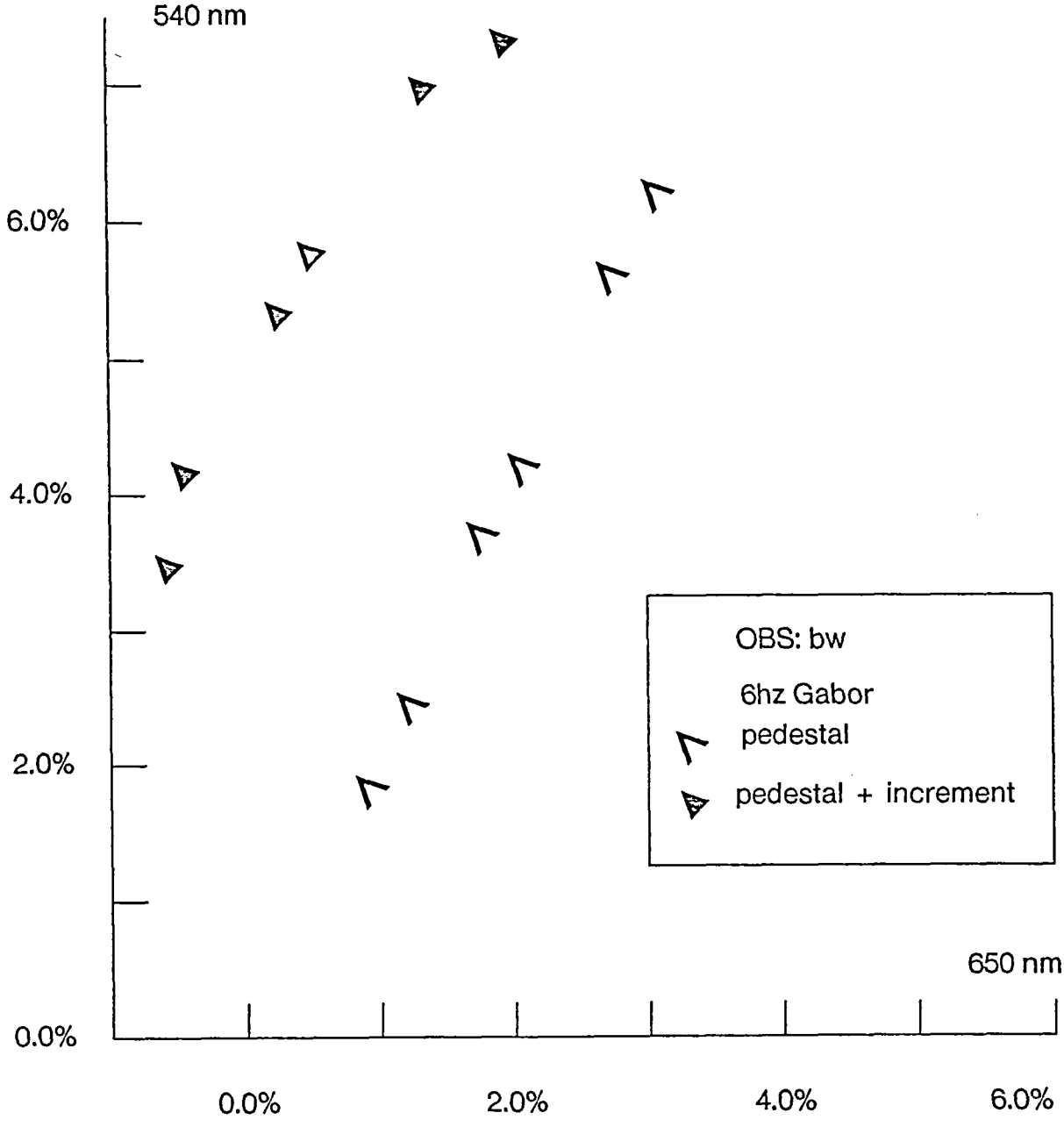
540 nm
6.0%
4.0%
2.0%
0.0%
650 nm
0.0%
2.0%
4.0%
6.0%
OBS: bw
6hz Gabor
pedestal
pedestal + increment

FIGURE 16c

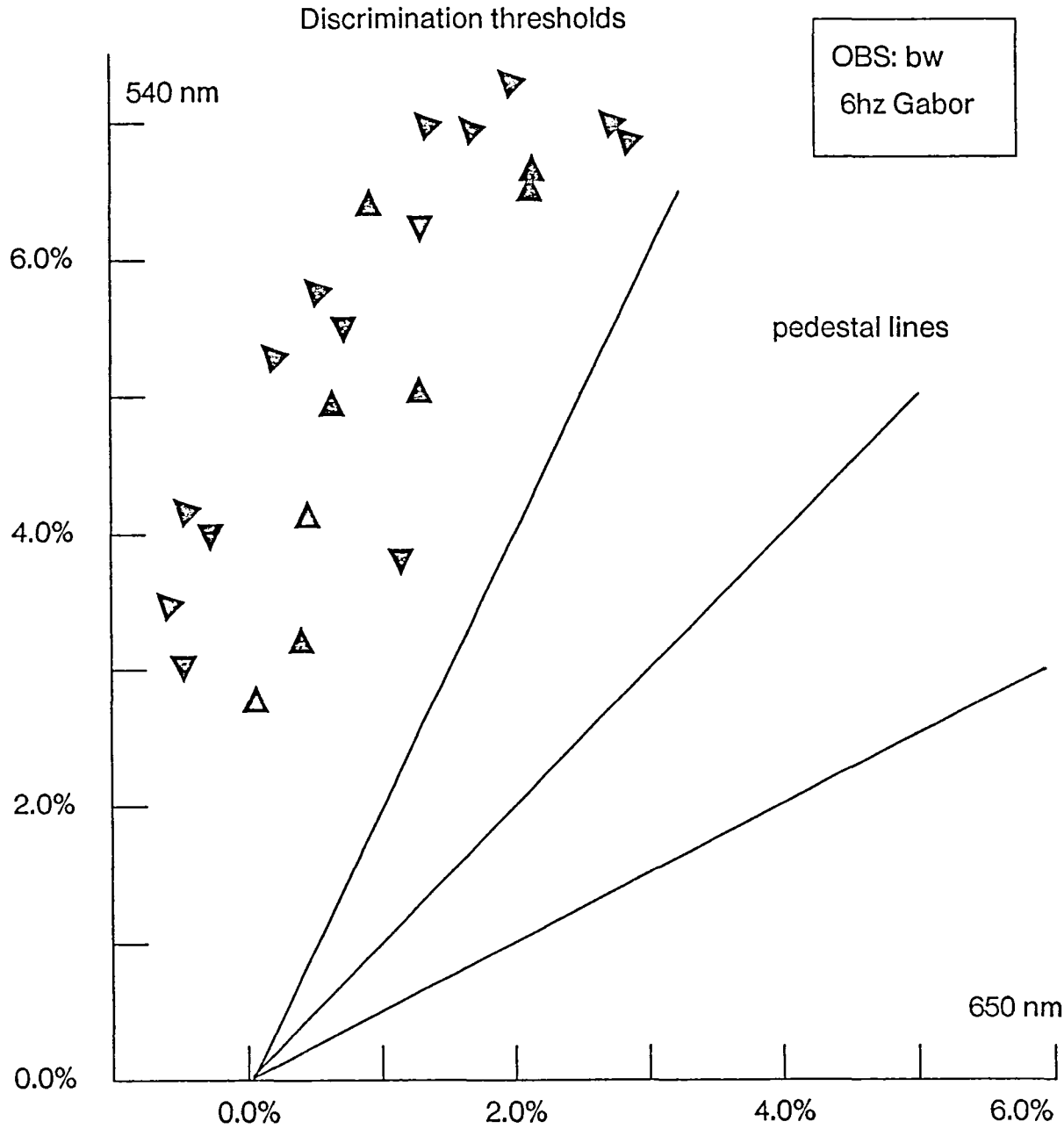
Discrimination thresholds
OBS: bw
6hz Gabor
540 nm
6.0%
4.0%
2.0%
0.0%
pedestal lines
650 nm
0.0%
2.0%
4.0%
6.0%

FIGURE 17

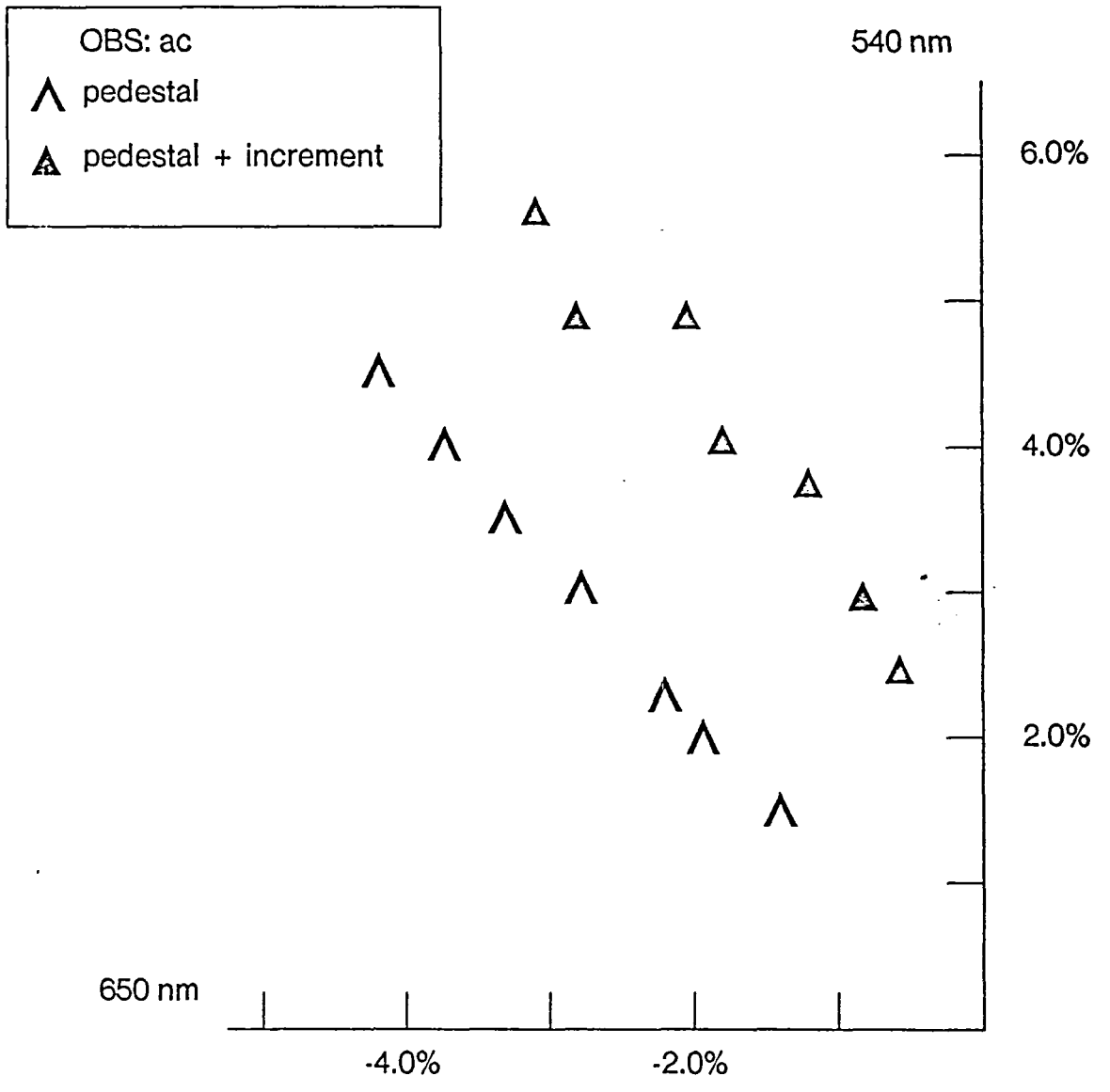
OBS: ac
pedestal
pedestal + increment
540 nm
6.0%
4.0%
2.0%
650 nm
-4.0%
-2.0%

FIGURE 18a

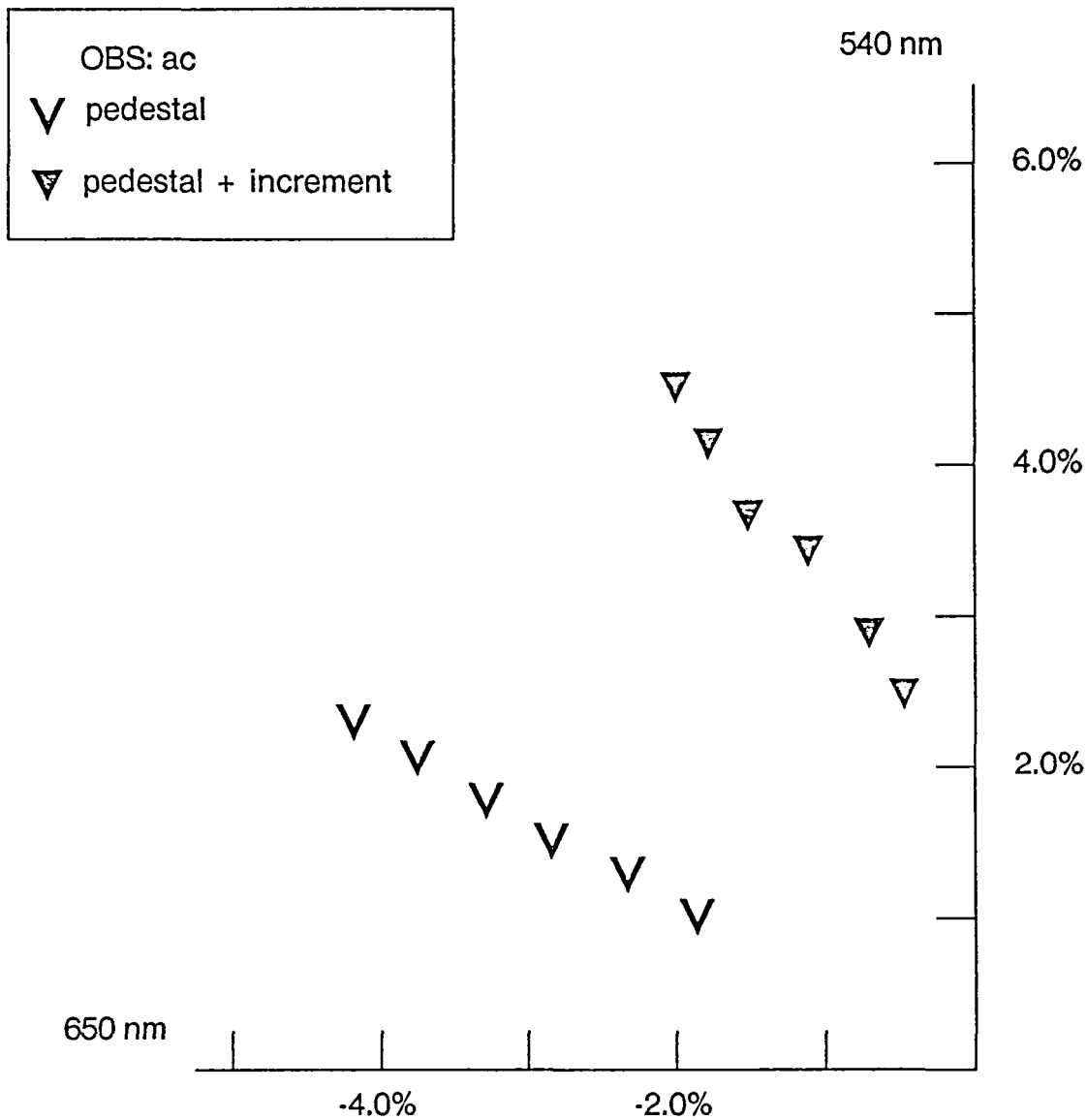
OBS: ac
pedestal
pedestal + increment
540 nm
6.0%
4.0%
2.0%
650 nm
-4.0%
-2.0%

FIGURE 18b

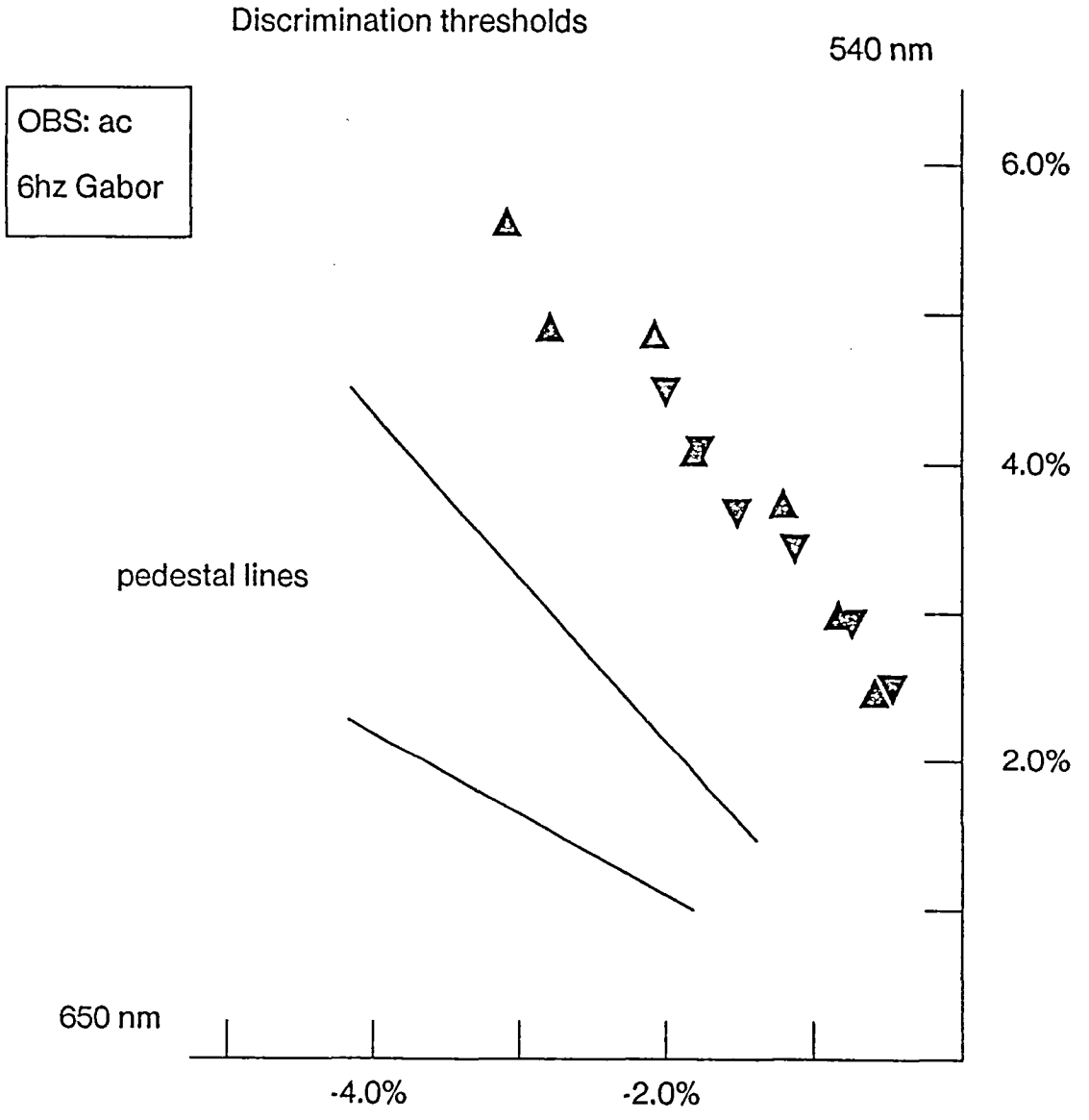
Discrimination thresholds
540 nm
OBS: ac
6hz Gabor
6.0%
4.0%
2.0%
pedestal lines
650 nm
-4.0%
-2.0%

FIGURE 19

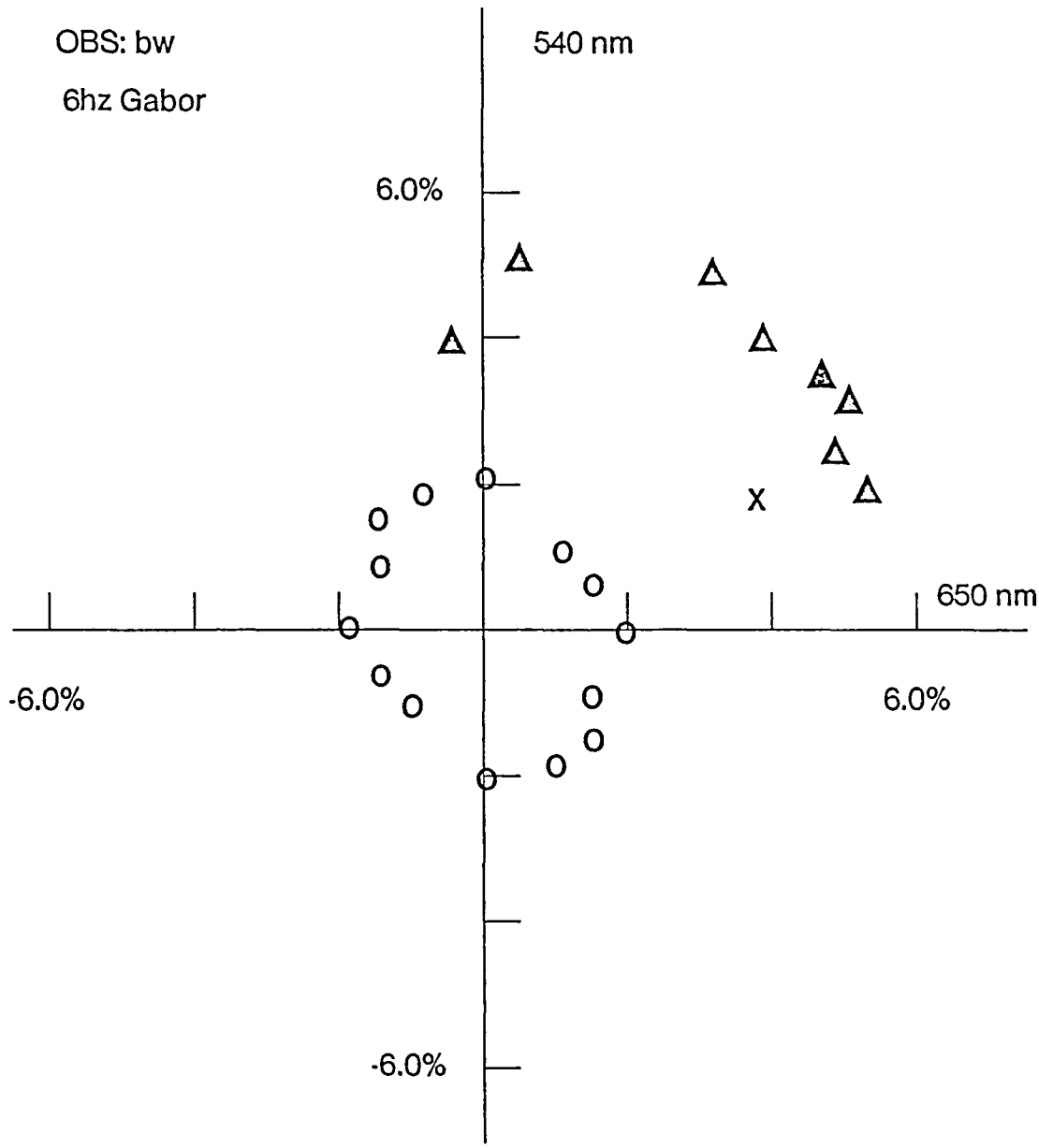

FIGURE 20

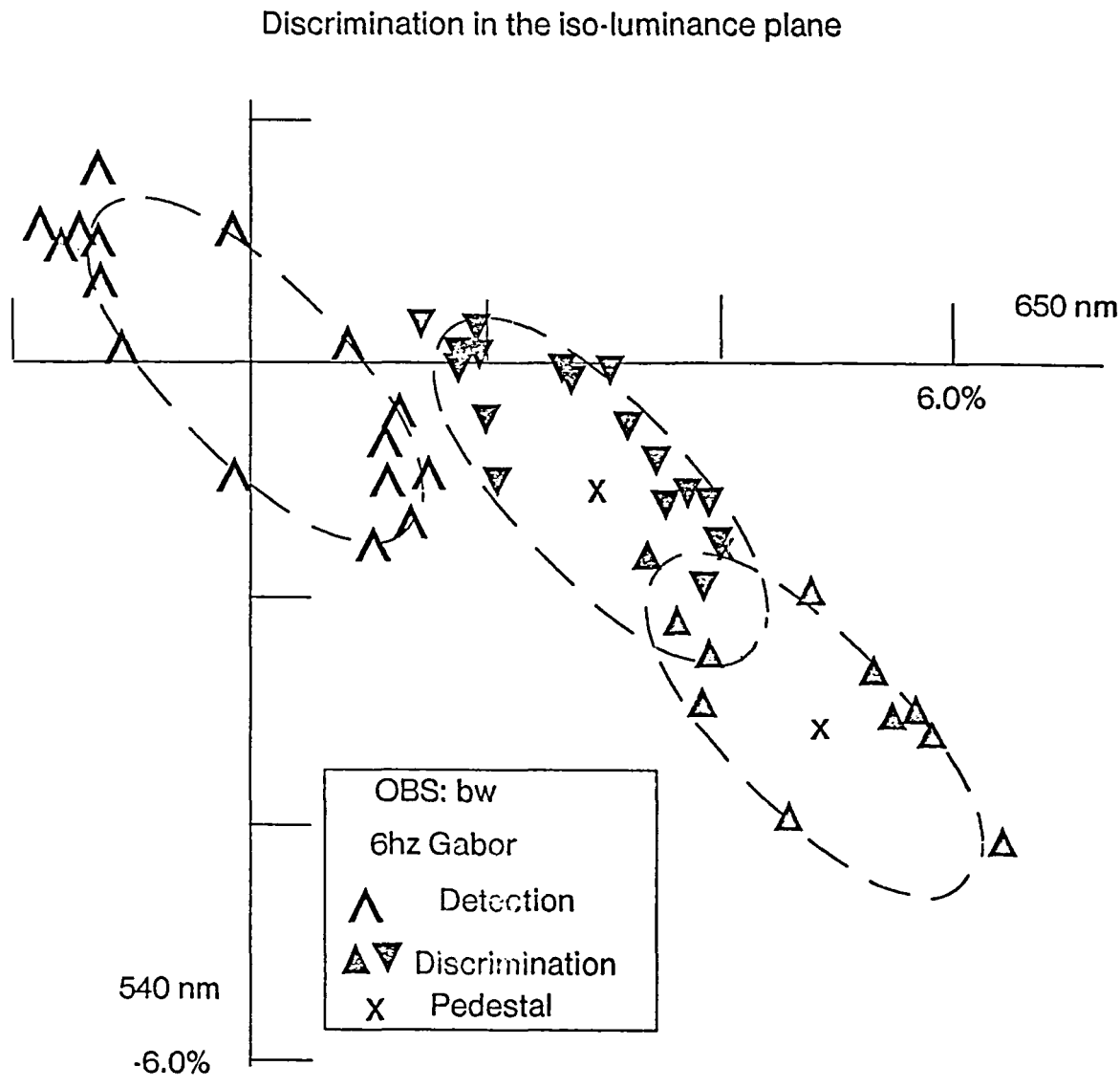
Discrimination in the iso-luminance plane
650 nm
6.0%
540 nm
-6.0%
OBS: bw
6hz Gabor
Detection
Discrimination
Pedestal

FIGURE 21

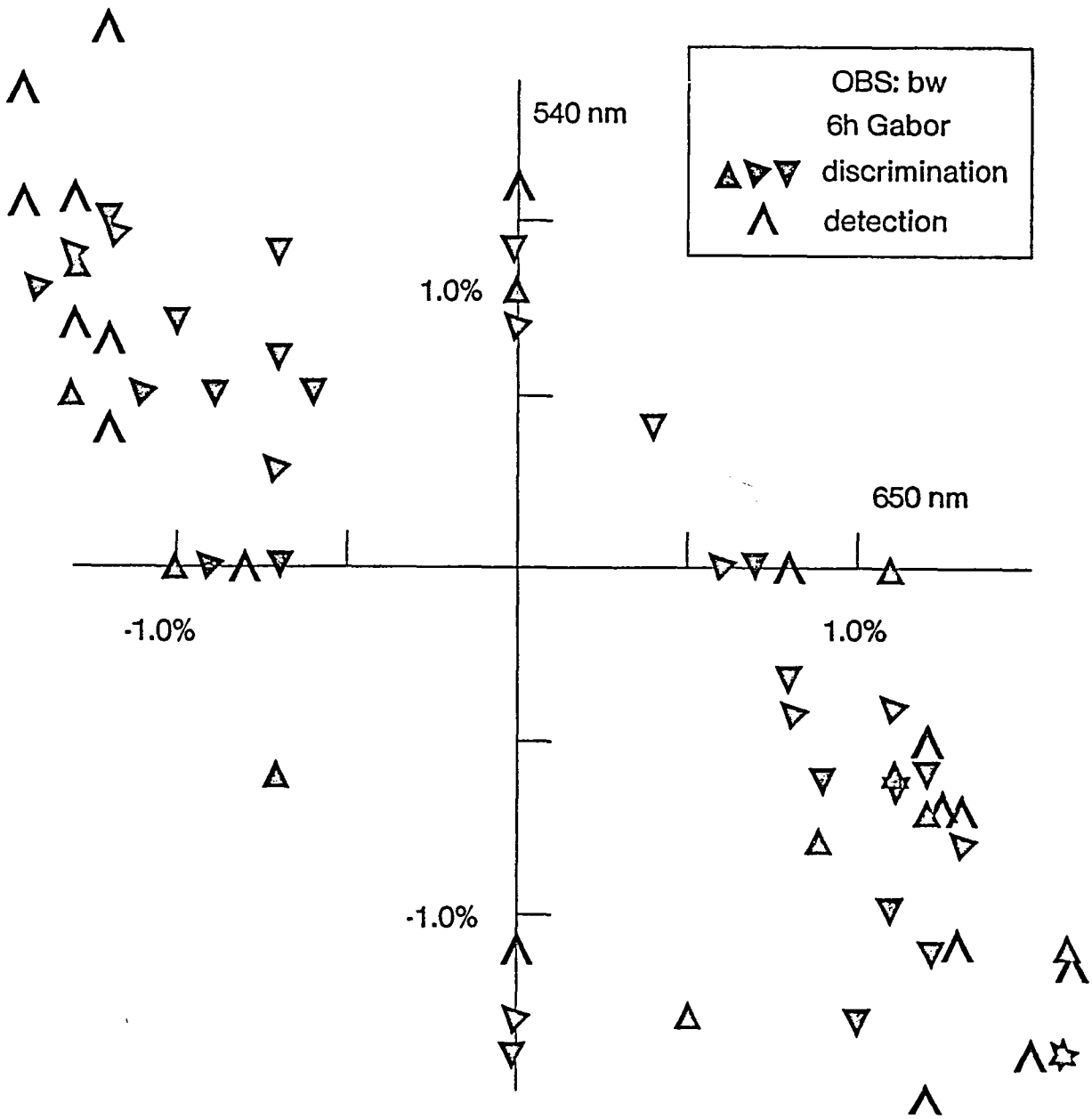
OBS: bw
6h Gabor
discrimination
detection
540 nm
650 nm
1.0%
-1.0%
1.0%
-1.0%

FIGURE 22

1. Report No.	2. Government Accession No.	3. Recipient's Catalog No.
NASA CR-3824		

4. Title and Subtitle	5. Report Date
Color Measurement and Discrimination	February 1985
	6. Performing Organization Code

7. Author(s)	8. Performing Organization Report No.
Brian A. Wandell	

9. Performing Organization Name and Address	10. Work Unit No.
Stanford University Psychology Dept. Stanford, CA 94305	T-4328
	11. Contract or Grant No. NCC2-44

12. Sponsoring Agency Name and Address	13. Type of Report and Period Covered
National Aeronautics and Space Administration Washington, DC 20546	Contractor Report
	14. Sponsoring Agency Code 505-35-31

15. Supplementary Notes

Point of Contact: David Nagel, ms 239-3, Ames Research Center, Moffett Field, Ca. 94035 FTS 448-6170 or 415-965-6170

16. Abstract Theories of color measurement attempt to provide a quantative means for predicting whether two lights will be discriminable to an average observer. When the observer's state of adaptation is held fixed, all color measurement theories can be characterized as follows. Suppose lights a and b evoke a responses from three color channels that we characterize as vectors, v(a) and v(b). The vector difference v(a) - v(b) corresponds to a set of channel responses that would be generated by some real light, call it &. According to theory a and b will be discriminable when & is detectable.

This paper reports a detailed development and test of the classic color measurement approach. In the absence of a luminance component in the test stimuli, a and b, the theory holds well. In the presence of a luminance component, the theory is clearly false. When a luminance component is present discrimination judgments depend largely on whether the lights being discriminated fall in separate, categorical regions of color space.

The results suggest that sensory estimation of surface color uses different methods, and the choice of method depends upon properties of the image. When there is significant luminance variation a categorical method is used, while in the absence of significant luminance variation judgments are continuous and consistant with the measurement approach.

17. Key Words (Suggested by Author(s))	18. Distribution Statement
Vision, Color Theory, Perception, Displays	Unclassified - Unlimited Subject Category 54

19. Security Classif. (of this report)	20. Security Classif. (of this page)	21. No. of Pages	22. Price*
Unclassified	Unclassified	80	A05

*For sale by the National Technical Information Service, Springfield, Virginia 22161 NASA-Langley, 1985

National Aeronautics and
Space Administration

Washington, D.C.
20546

Official Business
Penalty for Private Use, $300

THIRD-CLASS BULK RATE

Postage and Fees Paid
National Aeronautics and
Space Administration
NASA-451

POSTMASTER: If Undeliverable (Section 158 Postal Manual) Do Not Return